Advanced Methods for IDP and Refugee Camp Mapping with Very High Resolution Satellite Imagery

Magisterarbeit

zur Erlangung der Würde des Magister Scientiarum (M.Sc.)

Institut für Physische Geographie

Fakultät für Forst- u. Umweltwissenschaften

Albert-Ludwigs-Universität Freiburg

vorgelegt von

Martin Gayer

aus Mühlacker

Freiburg 02.07.2008

Erstbetreuer: Professor Dr. Rüdiger Glaser

Zweitbetreuer: Dr. Helmut Saurer

Declaration / Erklärung

I assure that the present thesis was carried out without external help and without using further than the stated sources. I also confirm that this thesis was not submitted to another examination board. All quotations are marked adequately.

Ich versichere, diese Magisterarbeit ohne fremde Hilfe und ohne Verwendung anderer als der angeführten Quellen angefertigt zu haben, und dass die Arbeit in gleicher oder ähnlicher Form noch keiner anderen Prüfungsbehörde vorgelegen hat. Alle Ausführungen der Arbeit, die wörtlich oder sinngemäß übernommen wurden sind entsprechend gekennzeichnet.

Freiburg, 01.07.2008

Martin Gayer

Acknowledgements

The thesis was carried out with the German Remote Sensing Data Centre (DFD) at the German Aerospace Centre (DLR) in Oberpfaffenhofen. In this context I would like to express my gratitude to Dr. Harald Mehl and Dr. Stefan Voigt who made this cooperation possible. For showing me the possibility of writing this thesis at the DLR I would like to deeply thank Professor Dr. Rüdiger Glaser

My special thanks I would like to express to my academic advisors Dipl.-Geogr. MSc (GIS) Olaf Kranz and Dr. Tobis Schneiderhan. Both were excellent supervisors who gave numerous critical comments as well as various ideas for structuring the present thesis. Further on, I would like to take the chance to thank the whole team of the unit *Environment and Security* at the DLR. They gave me a very interesting and nice time during my stay in Oberpfaffenhofen as well as vigorous support for all my problems. Many thanks to Christine Radestock for the good time in the bureau and all the professional support with ArcGIS. Also thanks to André Twele, Hendrik Zwenzner, Sandro Martinis, Alexandra Förster and Jens Kersten for their innovative ideas and conversations as well as the good times after work. For keeping me smiling and giving me positivity during all the time I would like to express my gratitude to Veronika Gstaiger. For pointing out corrections I would like to give my warmest thanks to Wiebke Emrich.

Last but not least, very special thanks go to my family and in particular to Anika Johnsdorf for the support, inspiration and patience I could always count on. Very special thanks go to my aunt Dorothea Miller for providing me with food and shelter during my whole stay.

I Summary

Due to natural and man-made disasters, worldwide millions of people are seeking shelter in camps. Most of these camps are under supervision of national and international relief organizations which are responsible for supplying the camps with basic necessities. Therefore, knowing the number of inhabitants is an essential aspect for the effective management of the logistics.

This study aims to show that very high resolution satellite imagery can be used for counting residential numbers by extractions of actual shelters in the camps. Based on recent publications, methods for shelter extraction were examined and modified. With images derived from IKONOS (1 m resolution) of two Refugee/IDP (Internally Displaced People) camps in eastern Chad a visual interpretation, three pixel-based approaches and one object-based analysis were tested. Additionally, a visual interpretation of images recorded by the new radar satellite TerraSAR-X was applied to show the possibilities for refugee camp mapping with spatially very high resolution radar. In this context, IKONOS and TerraSAR-X images were combined.

The pixel and object-based methods for shelter extraction were discussed with regard to their accuracy and time expenditure as well as the possibilities for their implementation in diverse crisis situations. Therefore an exhaustive accuracy assessment on users, producers and overall accuracy was performed. Moreover, the different characteristics of the images were discussed. It was shown that the overall accuracy of the different methods ranges from about 34% to 88%. This discrepancy is due to characteristics of the shelters in the two campsites and the diverse methods for extraction. The object-based approach turned out to be the most robust technique with regard to the transferability to other imagery. The combined method of IKONOS and TerraSAR-X showed a high potential for more precise techniques in shelter mapping for future approaches.

II Inhalt

Auf Grund von natürlichen oder anthropogenen Ursachen suchen weltweit Millionen von Menschen Schutz in Flüchtlingslagern. Dabei sind die meisten Lager unter der Aufsicht von nationalen oder internationalen Hilfsorganisationen, welchen die Verantwortung für die Versorgungen der Lager mit lebensnotwenigen Gütern obliegt. Dabei sind genaue Angaben über die Anzahl der Campbewohner ein wichtiger Aspekt um die Logistik möglichst effektiv zu gestallten.

Ziel dieser Arbeit ist es, Möglichkeiten aufzuzeigen, die zur Bevölkerungsabschätzung in Flüchtlingslagern an Hand der Extraktion von Unterkünften aus sehr hoch auflösender Satellitenbilder dienen.

Mittels der aktuellen Literatur wurden dafür unterschiedliche Methoden untersucht und modifiziert. Mit Hilfe von Satellitenbildern des Satelliten IKONOS (1m Auflösung) wurden je ein Flüchtlingscamp sowie ein Camp für Binnenvertriebene (Internally Displaces People, IDP) mit einer visuellen Interpretation, drei pixel-basierten Ansätzen und einer objektbasierten Methode untersucht. Zusätzlich konnte eine optische Interpretation von Radardaten des neuen TerraSAR-X durchgeführt werden um die Chancen von räumlich sehr hoch aufgelösten Radardaten zur Flüchtlingslagerkartierung zu analysieren. In diesem Kontext wurden die Aufnahmen beider Satelliten (IKONOS und TerraSAR-X) auch in Kombination gebracht.

Die pixel- und objektbasierten Methoden wurden auf ihre Genauigkeit, den Zeitaufwand und die Möglichkeiten zur Implementierung in diversen Krisensituationen ausgewertet. Eine umfassende Genauigkeitsanalyse mit der Hersteller-, Nutzer- und Gesamtgenauigkeit wurde durchgeführt und die Charakteristika der Satellitenbilder diskutiert.

Es konnte gezeigt werden, dass die Gesamtgenauigkeiten der Methoden zwischen 34% und 88% liegen. Diese Disparitäten gehen auf die unterschiedlichen Aufnahmen und angewandten Methoden zurück. Der objekt-basierte Ansatz zeigte sich in Bezug auf die Übertragbarkeit als die robusteste Methode. Die Kombination optischer Daten mit Radardaten stellte sich als der

Ansatz mit dem größten Potential für zukünftige Techniken der Extraktion von Behausungen von Flüchtlings- und IDPs anhand von räumlich sehr hoch auflösenden Satellitendaten heraus.

Index

III List of tables

IV List of figures

V List of abbreviations

ERTS – Earth Resources Technology Satellites

CAR – Central African Republic

DFD – German Remote Sensing Data Centre

DLR – German Aerospace Centre

GIS – Geographical Information System

IDP – Internally Displaced People

ISODATA – Iterative Self-Organizing Data Analysis Technique NGO

NGO – Non-Governmental Organization

NIR – Near Infrared

PCA – Principal Component Analysis

PGDS – Population Data Unit

QB – Quickbird

SAR – Synthetic Aperture Radar

SLR – Side-looking Radar

SRTM – Shuttle Radar Topographic Mission

TSX – TerraSAR-X

UN – United Nations

UNHCR - United Nations High Commissioner for Refugees

UNOSAT - United Nations Operational Satellite Applications Programme

UTM – Universal Transverse Mercator

VHRS – Very High Resolution Satellites

ZKI – Centre for Satellite Based Crisis Information

1 Introduction

The research of population or settlement mapping connected to imagery from space has been one of the basic topics since remote sensing developed in the 1960s. Photographs taken during the Gemini or Apollo missions were already used to estimate characteristics, like extents or densities of settlements (Tobler 1968). Since the start of the ERTS-1 (Earth Resources Technology Satellites) in 1972, these examinations have been continuously improved in the focus of population estimation, population growth and population movement. Arising from these scientific researches, the support of humanitarian relief organisations and the decision-making for policymakers with up-to-date geo-information have taken on greater significance in crisis situations and long-term monitoring over the last decades. Especially for relief organizations, it is of highest interest to respond quickly to natural and man-made disasters with adequate aid. During the recent years, numerous people died due to the limited efficiency of relief-operations, i.e. in Ethiopia, Rwanda, Burundi, Zaire and in the Sudan. (Dalen et al. 2000)

Today, an increasing number of relief organizations appreciate the value of geographical information delivered from earth observation satellites from areas where no adequate ground information is rapidly available. Scientific approaches for that are about all aspects of support in disaster situations. Rapid response is always needed when human lives are at risk. Eastern Chad's border region to Sudan was taken as the study area for this examination due to the complex crisis situation that is caused by war, remoteness and forced population movements in that area. Two exemplarily campsites are getting analysed via very high resolution satellite imagery – optical as well as radar data.

The overall objective of this thesis is giving support to the applied geographical sciences that are taking out researches for the maintenance in humanitarian disaster situations.

The thesis was conducted within the two projects LIMES and RESPOND. LIMES (Land and Sea Integrated Monitoring for Environment and Security) is an Integrated GMES-Project co-funded by the European Commission within the 6° Framework Programme. This project aims at the development of satellite-based services providing relevant information and decision-support tools in relation to

different domains. One of these domains is the organisation and distribution of humanitarian relief and reconstruction. RESPOND is an ESA GMES Service Element (GSE) that aims at improving access to maps, satellite imagery and geographic information. Several users of the humanitarian community are provided with mapping products such as Situation Maps and Damage Assessment Maps during urgent disaster situations to support the decision-making process. The Centre for Satellite Based Crisis Information (ZKI), which is a service of DLR's (German Aerospace Centre) German Remote Sensing Data Centre (DFD), is strongly involved into both projects. (DFD 2008)

The present thesis is structured into six chapters in the following way. At first, a state of the art about refugee camp mapping is described. Chapter 2 gives an overview about the area of interest in Chad and the situation of refugees and IDPs as well as the interconnections to humanitarian relief organisations. The principles of optical and radar remote sensing are presented in chapter 3. Methods for the mapping and extraction of shelters in campsites are getting illustrated in chapter 4 for optical data. The possibilities with radar data derived from TerraSAR-X are given in chapter 5. The discussion of the results and the recommendations due to their implementation as well as recommendations for future prospects are shown in chapter 6.

1.1 Purpose of the Thesis

The main objective of this thesis is to find adequate methods for the extraction of individual shelters in refugee and IDP camps in the border region Chad/Sudan with means of very high-resolution satellite (VHRS) imagery. Techniques for realization are visual interpretation, pixel-based classification and object-based analysis. These methods will be analysed in accuracy and time consumption and discussed regarding their appropriate implementation in complex crisis situations. The secondary objective is the analysis of additional features that can be extracted from the images that may be beneficial for relief organizations or helpful for policymakers (on the basis of provision of information).

Worldwide there are millions of refugees and IDPs due to various reasons like war, natural disasters and famines (see Chapter 2.2). On the African continent, numerous of these affected people are seeking for shelter in humanitarian campsites. Chad's border region to Darfur in Sudan can be seen as a representative area for various conflicts in the Sahel and Sub Sahel region or for other parts on the African continent due to the remoteness of the campsites and the complexity of the crisis situation (see Chapter 2). In Chad, hundred-thousands of people, living in refugee or IDP camps, need to be supported by humanitarian relief organizations.

To provide refugees with the basic requirements like food, water, medicine, sanitation or cooking facilities, the camp management needs highly accurate statistics on camp size, distribution of inhabitants and correct geographical location. Relief organizations, like the UNHCR, started to integrate satellite data into these calculations. The Handbook for Emergencies (UNHCR 2007, P. 154) in its third edition advises that:

> *"Knowing the size and profile of the refugee population is essential for an efficient and cost-effective operation and is at the core of UNHCR's protection mandate. Refugee registration will serve as the basis for various standards and indicator reporting […] Population estimates can also be obtained by calculating the total area of the camp, then counting shelters in a fraction of the camp, from which the population of the whole camp can be extrapolated. Alternatively, aerial photograph or satellite images may be used to count the number of shelters."*

This explicit recommendation to use satellite imagery from one of the world's leading relief organizations emphasizes how imported the research in this discipline has recently become, the extraction of individual shelters and infrastructure for population statistics in particular. Today, due to commercially accessible VHRS imagery, even features in the scale of few meters are cognisable and can be used to achieve such requirements.

1.2 Literature Review - Medium and high spatial resolution sensors within the context of refugee/IDP camp mapping

Generally, satellite pictures can be categorized in different ranges of spatial resolutions. That expresses the quality of the smallest object that could be

detectable in satellite imagery, particularly the smallest detail that can be distinguished by a sensor. Medium-resolution imagery ranges from 10-50 meters, high-resolution imagery goes from 4-10 meters, very high-resolution from 1-4 meters and ultra high-resolution goes below 1 meter. Furthermore, it is essential to know that the higher the resolution of the satellite sensor, the smaller the area that can be covered. (Ehlers et al. 2003)

The first applications for refugee camp mapping with satellite imagery started during the 1990s. Imagery from medium (i.e. Landsat 4/5/7) and high-resolution (i.e. Spot 4/5) sensors were used for different kinds of mapping. Available satellite sensors have to be balanced out between technical restrictions and the needs of the world's leading relief agencies because the size of detectable features is directly related to the spatial resolution of satellite imagery (Bjørgo 2002). The ENVIREF (Environmental monitoring of refugee camps using high-resolution satellite images) Final Report 2001 (Johannessen et al. 2001) was the first all-embracing paper dealing with these topics.

Several camps in different geographical locations were examined carefully with remote sensing techniques. Beside the surrounding infrastructure, vegetation cover and hydrologic features, mainly the geographical location and extent of the camps were mapped. The advantage of ENVIREF was the close collaboration of the remote sensing institutions Nansen Environmental and Remote Sensing Center (NERSC), Swedish Space Cooperation Group (Satellus) and Infocarto Spain together with the humanitarian relief organisation United Nations High Commissioner for Refugees (UNHCR)[1]. The needs of the humanitarian relief organisation were compared to the potential of remotely sensed data, combined with a cost-performance analysis (see Table 1).

The methods that were used to analyse the refugee camps were pixel-based interpretation and visual interpretation. Change Detection techniques via NDVI (Normalized Differenced Vegetation Index) and Image Differencing with imagery derived from different sensors were also tested. After an evaluation all these techniques were considered to be useful for coarse features but not for fine structures like footpaths, tents or wells. It was mentioned that no accuracy

[1] Further on, there were co-operations with International Federation of Red Cross and Red Crescent Societies (IFCR), Medecines sans Frontieres (MsF), Oxfam UK, Norwegian Peoples Aid (NPA) and Food for the Hungry (FHI).

assessments have been made. *"The only analysis that indicates the accuracy is an example of shelter estimation that was carried out based on the classification result"* (Johannessen et al. 2001, P. 21). This study was about counting shelters from two refugee camps in Nepal based on IKONOS 4 meter multi-spectral and 1meter panchromatic data. The numbers of shelters were compared to official UNHCR numbers and had an accuracy error between 3-10%. That extraordinary result is mainly a consequence from the accuracy assessment described like: *"The number of shelters within the […] camps was computed by dividing the total number of pixels allocated to the class 'House' on an expected average number of pixels per house."* (Johannessen et al. 2001, P. 21) However, these statistics entail a high uncertainty.

Due to the all weather capability and independency from sunlight, radar data is seen as an important source whilst emergency situations i.e. frequent cloud layers in the tropics and subtropics make it impossible for optical sensors to extract the required information. Settlements are very sensitive to radar microwaves, especially ones with many horizontal and vertical structures. In the 1990s, radar data from European Remote Sensing Satellites (ERS) were analysed to get information about refugee camps. Some of the first ERS-based studies about position and extent of refugee camps were made by Dalen et al. (2000) and Bjørgo (1999). Their examinations were based on visual interpretation and were limited to the detection of large objects due to the data's pixel-spacing of 12.5 meter.

Concerning the former resolution of the imagery derived from radar data, Dalen et al. (2000) recommended counting fine structures like tents and small residencies should be done when higher resolution radar imagery is available.

With the successful launch of the German TerraSAR-X (TSX) in June 2007, very high-resolution radar data became accessible and accordingly, these small objects might be detectable now. TSX provides very high spatial resolution radar images up to 1 meter resolution on the earth's surface.

Table 1: Benefits and limitations from the final ENVIREF report 2001, about adequate satellite data for refugee camp mapping. Source: (Johannessen et al. 2001, S. 40)

Satellite	Parameters	Benefits	Limitations
LANDSAT ETM	Vegetation cover, surface water	Large spatial coverage, High spectral resolution (7bands), large archive	Low spatial resolution, expensive data, copyright restrictions reduce possibility for data sharing
LANDSAT ETM+	Vegetation cover, surface water, infrastructure, camp location, settlements	Large spatial coverage, high spectral coverage (7 bands), panchromatic band (15m resolution), low data price (USD600), large archive, liberal copyright regulations allow for important sharing of the data	Low spatial resolution beside the pan-chromatic band
SPOT XS	Vegetation cover, surface water, infrastructure, camp location, settlements	High spatial resolution, medium spatial coverage	Low spectral resolution, expensive data, copyright restrictions reduce possibility for data sharing
IRS-1D	Surface water, infrastructure, camp location, settlements	Medium to high spatial resolution	Low radiometric resolution (low contrast), copyright restrictions reduce possibility for data sharing
ERS SAR	Camp location, settlements, digital elevation data	Operates independent of clouds and light, quite low data price	Difficult to interpret, copyright restrictions reduce possibility for data sharing
IKONOS	Vegetation cover, surface water, infrastructure, residences	Very high spatial resolution, medium high spectral resolution	Small spatial coverage, expensive data, copyright restrictions reduce possibility for data sharing

1.3 Literature Review - Very high resolution imagery within the context of refugee/IDP camp mapping

Bjørgo described the potential of optical VHRS imagery for relief organizations already in 1999 when medium and high-resolution imagery were not longer sufficient for more detailed information extraction.

In general, the availability of VHRS data offers new opportunities for many kinds of detailed mapping actions. After the launch of VHRS with spatial resolutions of 1 meter (IKONOS 1999) or even 60 cm (Quickbird 2001), data for detailed residential area analysis became available. Even small features like tents, huts and small houses appear clearly in the satellite images. Visual interpretation methods as well as pixel and object-based approaches for shelter extraction with VHRS imagery of fast growing informal settlements like shanty towns, squatter camps, favelas and slums were examined. For that, the extraction of footprints of residencies as well as their correct geographical localization is the benefit of the new sensor generation. The same methods were transferred to detailed analysis of campsites and tent cities within the context of humanitarian relief actions (Giada et al. 2003a; Uttenthaler et al. 2007).

Several case studies were applied to many different campsites all over the world. A very detailed research was taken by Giada et al. (2003b), who examined the refugee camp Lukole in Tanzania via pansharpened IKONOS images with 1 meter resolution. Visual interpretation and four computer-assisted procedures (two pixel-based and two object-based) for shelter counting were compared to each other in respect to their accuracy and time consumption. Visually interpreted data of the shelters provided the basis for reference data. These reference data were estimated out of 18 sample areas within the camp and then extrapolated for shelters per area over the entire camp. Because of these assumptions, further statistics showed an operational accuracy of 85% to 95% to all computer-assisted methods. Besides, an analysis with 1-meter pan-sharpened IKONOS data was performed for the Lukole camp. Lang et al. (2006) tested an object-based application and a mathematical morphology-based algorithm for the refugee camp Goz Amer in Chad with pan-sharpened Quickbird 0.6 meters for counting residencies. For ground reference, visually interpreted data were taken into account like in the studies of Giada. For quantification and comparison of these

methods, the extracted shelters were counted in grid-cells with an extension tool in ArcGIS. An accuracy assessment was applied to the results of Lukole camp only. The accuracy of the shelter extractions depending on the applied extraction method ranges from 65% for the morphological algorithm to 95% for the object-based approach for homogenous reflections of the structures of interest.

In 2007, Blaschke et al. mentioned the application of radar VHRS imagery of TSX in combination with optical VHRS data for more detailed information extraction regarding refugee camp mapping. However, till this day no respective appliance can be found in the current literature.

The studies that were taken out show that VHRS data coulc be used for refugee camp mapping. The results that got achieved are often based on accuracy assessments that contain several uncertainties due to the extrapolation of the visually counted shelters for reference data. There are very few studies were ground truth data was available because of the mostly dangerous circumstances in the campsites and their remoteness.

2 Study Area – Chad

Chad's overall situation is strongly interconnected to its geography, history and politics. Internal and external conflicts in Chad and its surrounding countries forced many people to flee from their place of origin (Chapter 2.3). Hundred-thousands of them are living in refugee or IDP camps in Chad's border region to Darfur/Sudan as well as in its neighbouring regions in southern Sudan.

2.1 Geography

Chad (see figure Figure 1) is located between 8° to 24° north and between 14° to 24° east in central Africa. The country with its 1,284,000 square kilometres is politically landlocked by Libya in the north, by Niger, Cameroon and Nigeria in the west, by the Central African Republic (CAR) in the south and by the Sudan in the east. Geographically, the Tibesti Mountains in the north of Lake Chad are a group of dormant volcanoes that reaches into southern Libya. The Ennedi Plateau and the Ouaddaï highlands dominate the scenery in the east and descend to the west through the Chad basin. The remaining country is mostly flat. (Auswärtiges Amt Deutschland - Federal Foreign Office Germany 2008).

Chad's vegetation and climate can be largely divided into the three zones of the Saharan, Sahelian and Soudanian region.

More than a third of the country's northern region is covered by the Saharan desert. This includes the Borkou-Ennedi-Tibesti prefecture along with the northern parts of Kanem, Batha, and Wadi Fira (formerly known as Biltine) prefectures. Just some oases and wells are dotted in this dry realm with a little annual rainfall average of less then three centimetres at Faya Largeau. Further southwards, rainfall increases to 350mm during July and August.

From Lac and Chari-Baguirmi prefectures in the east through Guéra, Ouaddaï, and the northern Salamat prefectures to the Sudanese boundary, the semiarid Sahel zone represents a climatic transition belt from the Saharian zone in the north down to the more humid Soudanian zone in the south. The vegetation changes from shrub to grass savannah following the increasing precipitation from north to south. In contrast to the rainy season during June to September, there is

almost no precipitation from October till May. To name an example, the Capital N'Djamena records a maximum annual average rainfall of 580 millimetres.
The Soudanian region consists predominantly of woodland savannah and deciduous forests. The humid zone extents to the southern prefectures of Mayo-Kebbi, Tandjilé, Logone Occidental, Logone Oriental, Moyen-Chari, and southern Salamat. Between April and October, the rainy season brings between 750 and 1,250 millimetres of precipitation, whereas the southwest is getting more rain then the remaining parts. (Collelo 1988)

2.2 History

After 60 years under French rule, Chad declared independence in 1960. In the following decades, the country experienced instability, corruption, military coups, misrule and low-intensity conflicts interspersed with civil war (IDMC 2007). Apart from the intergovernmental war between Libya and Chad (1978-1987), various rebel groups fought for leadership headed by small military and political elite like presidents, ministers or army officers. The ongoing conflicts between rebel groups in the north and governmental military in the south are more about ethnical and religious aspects rather than politics. The population in the south consists mainly of so-called black Africans, Animistics and Christians, whereas the north is dominated by Islamic Arabic Africans. Governmental and rebel groups often used France, Libya or the USA as assistant third parties for financing and the delivery of weapons. In return, France wanted to secure its economical and political interests in the region, the USA intended to protect its regional oil industries and Libya purposed to enlarge its territory to the south. In the context of the cold war, Russia also provided weapons for rebel groups to fight against western interests. In 1996, with the election of Idriss Deby for President, the conflicts calmed down but have continued till now. (Schicho 1999; Bailly 2004)
Chad is also affected by the tense situations of its neighbours Sudan and the Central African Republic. Chad and Sudan are blaming each other for supporting opposition rebel groups. (BBC NEWS 01.02.2008)

Figure 1: Map of Chad showing prefectures and neighbouring countries

Source: own design, modified raster and vector data from http://maplibrary.org/

2.3 Reasons for Displacement

Newest surveys from 2008 counted 11.4 million refugees and 26 million other internally displaced people worldwide.

As for Chad, hundred-thousands of people (Chapter 2.3.2) have been crossing the border from neighbouring Sudan due to the civil war, which started in 2003. Furthermore, over 140.000 internally displaced people are in Chad due to internal conflicts (Chapter 2.2) in Chad (UNHCR 26.03.2008; UN NEWS CENTRE 18.03.2008). An overview about the status of refugees and IDPs (Chapter 2.3.1) and about the current situation in Chad shall be given in this chapter.

2.3.1 Definition of Refugee & IDP

A refugee is defined by the Refugee Convention in Geneva from 1951 and then modified 1967 as:

> *"A person who owing to a well-founded fear of being persecuted for reasons of race, religion, nationality, membership of a particular social group or political opinion, is outside the country of his nationality and is unable or, owing to such fear, is unwilling to avail himself of the protection of that country; or who, not having a nationality and being outside the country of his former habitual residence as a result of such events, is unable or, owing to such fear, is unwilling to return to it." (United Nations Geneva, 28 July 1967, Article 1)*

The status of Internally Displaced Persons (IDP) is still not officially defined. IDPs can be defined as Refugees within their country of origin. However, there are definitions that clearly show the circumstances that IDPs are facing. One approach for definition was made in the United Nations Guiding Principles on Internal Displacement. Here, IDPs are considered:

> *"[…] persons or groups of persons who have been forced or obliged to flee or to leave their homes or places of habitual residence, in particular as a result of or in order to avoid the effects of armed conflict, situations of generalized violence, violations of human rights or natural or human-made disasters, and who have not crossed an internationally recognized State border." (Representative of the Secretary-General on Internally Displaced Persons (United Nations et al. 1998)*

This definition will be taken as the standard characterisation of IDPs in this thesis.

2.3.2 Refugees and IDPs

Plenty of ethnic groups or tribes with different cultural or ethnical backgrounds and relations to each other live in Chad and its neighbouring countries. Please note that the following descriptions of conflicts are very general. Unquestionably, the conflicts are much more complex but describing further details would go beyond the scope of this thesis. Detailed information about conflicts in Chad and neighbouring Darfur can be found in Strube-Edelmann (2006) and Köndgen (2004).

Since mid-2005, heavy conflicts in Central Africa Republic (CAR) have been taking place. The north of CAR can be seen as a lawless region due to the presence of different groups of bandits and rebels. Ongoing fights between troops of CAR and rebel groups in the north of the country caused the internal displacement of more than 212.000 people and forced 80.000 to flee in the neighbouring countries Chad, Cameron and Sudan. Until today, Chad is hosting 45.000 refugees from CAR in its south, but the number is still increasing (ReliefWeb 26.09.2007; UN NEWS CENTRE 18.03.2008).

In 2003, a civil war between ethnic Arab and ethnic African Chadian started in eastward neighbouring Sudan and affects the eastern part of Chad as well. This conflict is more about ethnical reasons and the distribution of natural resources rather than religious motivation; all parties are Islamic. Since 2003, more than 240.000 refugees from Sudan have been looking for relief and shelter in several campsites near the frontier to Sudan in eastern Chad (BBC NEWS 01.02.2008).

Additionally, there are about 140.000 internally displaced people caused by interior conflicts (see chapter 2.2) on one hand, and by militia groups entering from the Darfur region and CAR into Chad on the other hand (UN NEWS CENTRE 18.03.2008). A refugee camp and an IDP site in Chad near the Sudanese border are examined each by satellite imagery in this thesis.

2.4 Refugee and IDP camps in Chad

In eastern Chad, there are 12 refugee camps for mainly Sudanese refugees and over 20 Chadian IDP sites (see Figure 2). All campsites are under the patronage of UNHCR, which aims at assuring humanitarian standards through six field

offices and the finance of the humanitarian aid. Permanent information for policy-makers about the current situation is also an important duty for the UN refugee agency. Additionally, the camps are managed in cooperation with several Non-Governmental Organizations (NGOs) like the Red Cross, InterSOS or CARE etc. (UNHCR CHAD/DARFUR EMERGENCY March 2008; UNHCR 06.06.2007)

2.4.1 Phases and Organisation in Camps

In general, a refugee camp can be seen as an accumulation of tents with some food distribution facilities in-between. But with respect to the extent and the population living in these camps, it is more like a mid-size village that has to be built from scratch. (Dalen et al. 2000). Relief agencies usually face two possible situations: Camp-planning can be done prior to the arrival of refugees, for example if they are transferred into a camp or the camp is already established by refugees. That means that the site was built up by refugees before the arrival of relief agencies. However, a poorly planned or spontaneous refugee camp can become a very pathogenic place after some days due to a high number of people and poor hygienic conditions. Sanitation and healthcare have to be provided instantaneously to prevent the transmission of diseases. Also, appropriate shelters are needed for privacy and to cover from rain, wind and sun (UNHCR 2007a). In this context, it is not revisable how many camps are planned or built up spontaneously in Chad. The campsites in the mentioned region in Chad were examined in homogeneity of the adjustment of shelters via Google Earth, where many camps are displayed with VHRS imagery. It was found out that the sites are both, homogenous and inhomogeneous regarding the arrangement of shelters but from that no explicit conclusions can be drawn without any ground truth. The availability of natural resources is one of the essential concerns in refugee or IDP camps. In many cases, the population living in the camp is even higher than the number of residents in the surrounding villages. Thus, nearby villages should not face disadvantages because of a campsite, i.e. due to the occupation of land, the collection of firewood or a decreasing groundwater level. That has often caused tensions between villagers and refugees in the past. To avoid worse standards of living, neighbouring residents should be permitted to use i.e. medical services, schools and other benefits of relief organizations in campsites. All that must be

ensured over a long period. The mean lifetime of a refugee camp is seven years but it goes up to twenty years in some cases i.e. eastern Sudan. The conflict in the border region between Chad and Sudan has been going on since 2003. (Dalen et al. 2000; Cue 2007).

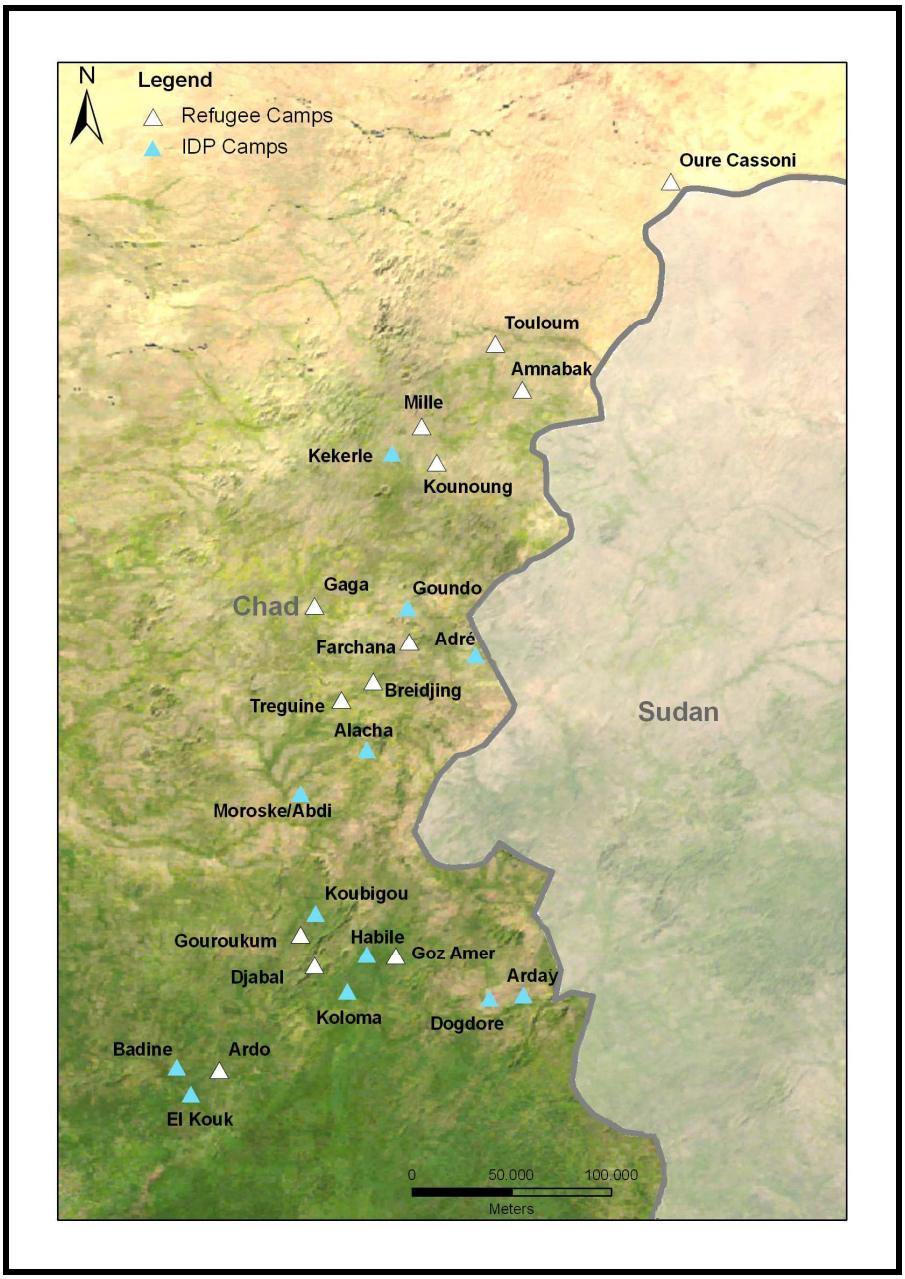

Figure 2: Several refugee and IDP sites placed in eastern Chad near the border to Sudan.

Source: own design, information about camp location derived from http://www.unhcr.org/cgi-bin/texis/vtx/chad (15.05.2008); modified raster and vector data from http://maplibrary.org/ (15.05.2008)

2.4.2 The Need for Geo-information

Johannessen et al. (2001) stated that spatial information is essential for effective camp management and decision-making. According to the required geo-information, humanitarian relief actions for refugee and IDP camps can be divided into three different phases:

- In an *emergency* phase, it is of vital importance that at least basic data of the area of interest are rapidly available i.e. topographic maps. Depending on the emergency, information about existing or potential camp sides, residencies, water resources, airfields, land use and roads are required. In order to manage such cases with good logistics, up-to-date maps of the affected region can provide very useful information.

- *Care* and *maintenance* of camps is realised by updating information about the structure, population and population density of the camp. Due to the increase and decrease of their population, refugee camps are highly dynamic settlements. People also move within the camp, i.e. to get closer to relatives.

- During the *repatriation* phase, awareness of the environmental circumstances in the refugees' area of origin is required i.e. information on potentially available land for agriculture is therefore of high interest. Furthermore, potential long-term environmental impacts have to be addressed during this phase.

Within the scope of these issues, UNHCR - Population Data Unit (PGDS) published 2005 a *Step-by-Step Guide to Mapping a Refugee Camp*. In this study, residential areas, sectoral facilities and roads have been identified as most important features for the management of a camp. The required information can be derived from the analysis of satellite imagery and additional field data. Remote sensing software and Geographical Information Systems (GIS) provide extensive capabilities for processing and analysing spatial data. Within the scope of this

thesis, it is intended to focus on the residential areas. The application for remote sensing methods regarding the three phases is discussed in detail in chapter 6.

2.4.3 Remote Sensing for Refugee Camp Mapping

Generally, remote sensing can be a powerful instrument in numerous mapping applications. Specifically, remote sensing can be used to provide detailed information about refugee camps to relief organisations like UNHCR, CARE or Red Cross who are able to handle such data. Calculating efficient statistics out of the provided information is therefore one of the principal conditions to assure the refugees' supply with basic requirements like food, water, medicine, sanitary or cooking facilities as well as security. As mentioned above in the introductory chapter, the Handbook for Emergencies (UNHCR 2007a, P.156) focuses in its third edition on information about the population:

> *"Knowing the size and profile of the refugee population is essential for an efficient and cost-effective operation […] Population estimates can also be obtained by […] satellite images […] to count the number of shelters."*

Remote sensing provides useful information additionally to data collected in field observations. Satellite imagery offers the opportunity to get an overview of campsites and an intuitive assessment about the in situ circumstances can be done through visual interpretation. Using very high-resolution imagery, population and population density can be estimated by the number of dwellings, such as tents or huts. (Giada et al. 2003a).

One of the benefits of a satellite image is its objectivity. Earth observation satellites actually record a picture of the present shape of the worlds' surface. Thus, nobody can argue that the data has been manipulated, as can be argued if biased individuals or companies collect field information in remote areas where no proof can be taken. Due to this, satellite data become a valuable source for policy-makers or donors when presenting the actual situation in the view from above. Of course, also satellite data can be modified and manipulated towards the intended results but the original digital data stays objective and can be evaluated again. Physical aspects for modifications on satellite images could be natural intermediate effects between the sensors and the sensed objects in consequence

of atmospheric effects like i.e. scatter effects due to water vapour (see Chapter 3.2) (Bjørgo 2002; Lillesand et al. 2004).

3 Principles of Remote Sensing

In this thesis, advanced techniques for the extraction of dwellings in refugee camps were tested and compared to each other. There are several methods to extract man made structures like tents or shelters from a satellite image but due to different earth observation satellites and their different sensors, it is of high interest to know about circumstances that possibly influence the information content. In general, remote sensing refers to the performances of observing and recording objects or events at distant places. In remote sensing, sensors are not in direct contact with the objects or events being observed. The information needs a physical carrier to travel from objects or events to sensors through an intervening medium. The electromagnetic radiation is normally used as an information carrier in remote sensing (Lillesand et al. 2004). Sabins (1978, P.1) defined it as*:*

> *"Remote sensing may be broadly defined as the collection of information about an object without being in physical contact with the object. Aircraft and satellites are the common platforms from which remote sensing observations are made. The term remote sensing is restricted to methods that employ electromagnetic energy as the means of detecting and measuring target characteristics."*

Remote sensing can be divided into passive and active systems, whereas passive systems principally receive wavelengths of radiation without formerly having transmitted them, i.e. multi-spectral sensors receive reflected sunlight. On the other hand, active systems send out signals and then capture the reflections, i.e. Synthetic Aperture Radar transmitting and receiving electromagnetic microwaves. With the focus on optical and radar sensors, the basic principles of physical interactions between sensors and sensed objects should be described succinctly in this chapter.

3.1 The Electro-magnetic Spectra

To get an understanding about the function of remote sensing sensors and the media that transports the information of the sensed objects, it is important to be familiar with the electro-magnetic spectra.

Visible light is the most recognised electromagnetic energy from the electromagnetic spectrum, but other forms like radio-, heat-, infrared, or X-ray waves are also represented within the electromagnetic spectra. All electromagnetic waves travel with the speed of light through space in the form of periodic disturbances of electric and magnetic fields (see Figure 3). Frequency and wavelength characterize an electromagnetic wave. These two attributes are related to the speed of light by the equation,

$$c = f \bullet \lambda$$

λ = wavelength

c = speed of light

f = frequency

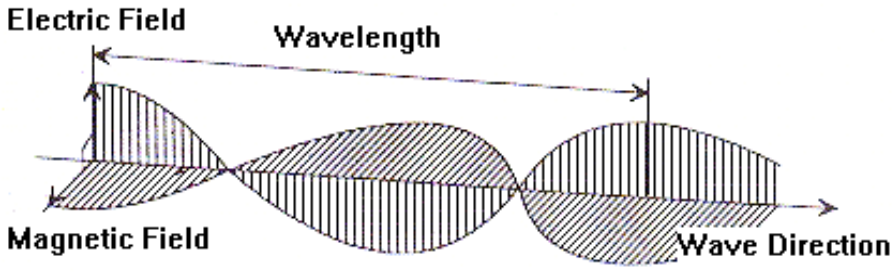

Figure 3: Electromagnetic wave within the magnetic and electric field.
Source: http://www.crisp.nus.edu.sg/~research/tutorial/em.htm#visbands (23.03.2007)

Furthermore, the categorization of electromagnetic waves is done by their wavelength location within the electromagnetic spectrum (see Figure 4). Important ranges for earth observations range from ultraviolet (3 to 400 nm), visible light (460 nm to 760 nm), and infrared (0.7 to 300 µm) up to microwaves (1 mm to 1 m). (Lillesand et al. 2004). A further subdivision of radar-waves is given in chapter 3.5.

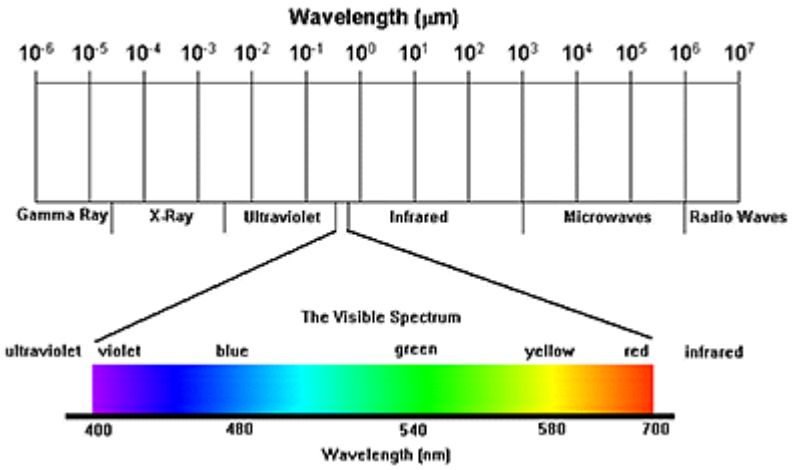

Figure 4: The electromagnetic spectrum and the visible range.

Source: http://www.crisp.nus.edu.sg/~research/tutorial/em.htm#visbands (23.03.2007)

3.2 Effects of the Atmosphere

All electromagnetic waves detected by a remote satellite sensor pass through the atmosphere. Depending on wavelength and distance from the objects to the sensors, the atmospheric layers cause wavelength-dependent absorption and scattering of radiation.(Lillesand et al. 2004).

Scattering is mainly caused by particles and water vapour and is divided into Rayleigh scatter and Mie scatter. Rayleigh scatter is characteristic for the interaction of atmospheric molecules and particles that have a smaller diameter than the correlating wavelength. Shorter wavelengths are generally more affected due to the cause, that Rayleigh scatter is inversely proportional to the fourth power of wavelength. This kind of scatter is mainly responsible for the blue sky and also for bluish “haze” in imagery. Further on, Mie scatter as the most common impact is not strongly wavelength-dependent and can be described as the illumination of the sky itself or white light from clouds, mist and fog caused by particles, dust and water vapour. Thus, it depends on the geographical position of the sensed objects, how much these effects corrupt the quality of imagery, i.e. regarding water vapour, there is more atmospheric impact over rainforest than over desert (Lillesand et al. 2004).

Some of the atmospheric effects can be reduced with special software before the images are subjected to further analysis and interpretation. For the used images

in this thesis, an atmospheric correction was not possible due to the fact that the images were delivered from European Space Imaging in a pan-sharpened format, where no scientific atmospheric correction is possible afterwards.[2] Fortunately, the images show no cloud cover, which would be a strong impact.

Imagery received from radar satellite data is mostly, depending on their wavelength, not affected by atmospheric impacts due to the capability of microwaves of penetrating haze, light rain and clouds (Lillesand et al. 2004).

3.3 Pre-processing of Satellite Data

Before an image can be used for data analysis, several steps of correction have to be processed. The term *pre-processing* refers to rectification procedures for the geometry and radiometry of raw satellite data and the presence of noise. Geometric distortions emerge due to the earth's curved surface, the movement of the satellites and oblique viewing angles of the sensors. The goal is to put all image elements into their correct geographical position and, if required, also into certain map projection i.e. Universal Mercator Projection (UTM). The radiometric correction aims for the minimisation of the impacts of such factors as scene illumination, atmospheric conditions (see chapter 3.2), viewing geometry, and sensor characteristics. In addition, noise removal should correct unwanted disturbance coming from malfunctions of detectors or failures in the chain of analogue and digital signal processing.

Every satellite sensor has its own characteristics, which have to be taken into consideration if the corrections are realised by an analyst. However, most ground stations deliver satellite data at different processing levels to the end-user that have already passed through certain pre-processing. (Albertz 2001; Lillesand et al. 2004)

All used satellite data in this thesis were delivered by data providers with a geometric correction and high spatial accuracy. The projections of all images came in UTM. Noise in the imagery was not detectable and radiometric corrections were processed.

[2] Information through a conversation with Dr. Rolf Richter from the German Remote Sensing Data Centre (DFD).

3.4 Optical Sensors

Satellites with optical sensors detect visible, near infrared (NIR) and shortwave-infrared radiation as the sunlight reflects form targets on the ground (passive system). Every object on earth has a spectral reflectance within the electromagnetic spectrum which can be differentiated by an optical sensor collecting the reflection. Optical sensors are often defined by their resolution from medium, high, very high and ultra high due to the spatial resolutions as was described in chapter 1.2. Generally, the spectral resolution decreases with the increase of spatial resolution for most satellite sensors. This means, a very high-resolution sensor records less bands in the electromagnetic spectra than a medium-resolution sensor. For the investigation of the campsites in Chad, VHRS imagery was determined as adequate data for the purpose of shelter mapping due to the high-spatial resolution.

3.4.1 Multi-spectral & Panchromatic Sensors

Panchromatic imaging systems are single channel detectors measuring the brightness of a large range of radiation, mostly the visible to NIR (approx. 0,4 to 0,9 µm) but due to the single sensor detection the information about the colour gets lost.

Multi-spectral imaging sensors collect radiation within some narrow wavelength bands like blue, green, red, up to infrared. The resulting data is a multi-layer imagery that contains spectral (colour) and brightness information for each channel.

Physical aspects concerning different sensors lead to a higher resolution for panchromatic imagery as for multi-spectral ones. (Lillesand et al. 2004)

3.4.2 Image Enhancement

The aim of image or data enhancement is to improve the interpretation for distinguishing features in a scene. The techniques are largely divided into radiometric enhancement, spatial enhancement and spectral enhancement.

- Radiometric enhancement chance individual pixel values in the picture to improve the contrast ratio on an image, i.e. for radiometric enhancement a histogram equalization stretch was applied. That redistributes pixel values, so that there are approximately the same numbers of pixels with each value within a range and for that advance the contrast.

- Spatial enhancement modifies an image pixel value based on the values of the surrounding pixel's brightness. For spatial enhancement, the most important improvement, the resolution merges of the multi-spectral image with the pan-sharpened image was already done by European Space Imaging. Convolution filters like edge enhancement or high pass were also tested.

- Spectral enhancement is used to transform the values of pixels from multi-band images to compress band-information that is similar, extract new bands that are more interpretable or apply mathematical transformations and algorithms. The principal component analysis is a frequently used method to transform a set of correlated variables into a new set of uncorrelated variables in order to reduce the data and enhance the contrast. (Lillesand et al. 2004; ERDAS 2005)

Several other techniques of the three described image enhancements were tested in this study to improve the imagery for the users' eye. Results that were achieved are discussed in chapter 4.

3.4.3 IKONOS

With the launch of the American IKONOS satellite on September 24, 1999, very high-resolution imagery became commercially available for the first time.
The sun-synchronous orbit of IKONOS makes a global coverage between the 82° latitude north and south available. That provides availability on mid-latitude areas with a daily revisit at 45° obliquity, 3-day revisi t at 26° obliquity, 11-day revisit at 10° obliquity, and 141-day revisit at 1° obliquity. IKONOS collects 1-m panchromatic images and 4-m multi-spectral images that can be ordered and

used for mapping, monitoring, and development. Geo images are available in different band combinations. Panchromatic (black and white), multi-spectral (near infra red, red, green and blue,) and panchromatic-sharpened (colour with a higher resolution than regular multi-spectral image) are the standard products. The data is usually provided orthorectified with an UTM projection (Dial et al. 2003).[3]

For this study, the following two datasets of the IKONOS sensor were taken regarding to the displayed campsites that are comparable to similar camps in the region. The high spatial resolution was considered to be more beneficial than a high spectral resolution as the aim is to identify small features like shelters.

Table 2: Dataset for IDP camp Koubigou

Creation Date:	22.10.2007
Processing Level:	Orthorectified
Image Type:	PAN/MSI (pan-sharpened)
Interpolation Method:	Cubic Convolution
Map Projection:	Universal Transverse Mercator
Zone Number:	34 North
Datum:	WGS84
Product Order Pixel Size:	1 meter
Scan Azimuth:	0.01 degrees (foreward)
Nominal Collection Azimuth:	255.6277 degrees
Nominal Collection Elevation:	67.83876 degrees
Sun Angle Azimuth:	140.7604 degrees
Sun Angle Elevation:	66.48870 degrees
Acquisition Date/Time:	2007-10-09 09:23 GMT
Percent Cloud Cover:	0

[3]Further information in *IKONOS satellite, imagery, and products* (Dial et al. 2003)

Table 3: Dataset for Refugee Camp Amnabak

Creation Date:	19.10.2007
Processing Level:	Orthorectified
Image Type:	PAN/MSI (pan-sharpened)
Interpolation Method:	Cubic Convolution
Map Projection:	Universal Transverse Mercator
Zone Number:	34 North
Datum:	WGS84
Product Order Pixel Size:	1 meter
Scan Azimuth:	180.01 degrees (reverse)
Nominal Collection Azimuth:	250.8810 degrees
Nominal Collection Elevation:	87.95408 degrees
Sun Angle Azimuth:	139.2777 degrees
Sun Angle Elevation:	64.33498 degrees
Acquisition Date/Time:	2007-10-06 09:13 GMT
Percent Cloud Cover:	0

3.4.4 Quickbird-2

After the launch failure of Quickbird-1, the American Quickbird-2 (QB) was launched successfully on October 18, 2001. The spatial resolution of the data is up to 61 cm panchromatic and up to 2.4 m multi-spectral at nadir. With that resolution, the QB panchromatic sensor already comes into the range of ultra high-resolution sensors (Ehlers et al. 2003) but is commonly named VHR imagery. The revisiting time for QB ranges among 1-3.5 days with an off-track viewing angle of +/- 30°. The recorded spectral ban ds are similar to the ones from the IKONOS sensor (see above) with just slight differences, which makes the data of both sensors comparable. To sum it up, the products of QB are quite the same as those from IKONOS and for that, further analysis of QB images could be taken into account for refugee and IDP camp mapping. [4]

4 For additional information, visit the website http://www.digitalglobe.com/index.php/85/QuickBird or http://www.eurimage.com /products/quickbird.html (27.05.2008).

3.4.5 Advantages and Limitations of VHRS

The benefits of optical remote sensing are generally the same for most sensors and differ only in terms of advantages or disadvantages of diverse sensor resolutions. In Lillesand et al. (2004), Sabins (1978), Albertz (2001) and other literature about remote sensing principles, following advantages for the use of optical remote sensing are exposed:

- VHRS imagery has a spatial resolution, where objects within the 4 to 1 meter range can be identified.
- Survey of inaccessible or dangerous regions, e.g. Antarctica or war zones can be conducted without direct contact.
- It is an inexpensive and fast method of constructing base maps in the absence of detailed land surveys.
- The data can be combined with other geographic coverage in Geographical Information Systems.
- It is a relatively cheap and rapid method of acquiring up-to-date information over a large geographical area.
- Remote sensed data can be multi-used interdisciplinary from different scientific backgrounds with different scientific goals.
- Raw data remain objective in contrast to personal estimations from ground survey.

On the other hand, disadvantages are the following:

- The high spatial resolution limits a high spectral resolution for most sensors. VHRS sensors mostly range from one to four channels.
- The data is never a direct sample and should be calibrated through ground truth if the area is accessible.
- The data must go through several sophisticated pre-processing steps i.e. it must be geometrically corrected and geo-referenced.
- Atmospheric effects can manipulate the image i.e. cloud cover (see chapter 3.2)

- Great experience in image interpretation by the analyst is required in order to interpret an image correctly.

3.5 Radar Data

Radar is the acronym for *radio detection and ranging* and has a large field of use. A radar system transmits electromagnetic waves (see Chapter 3.1) in the microwave spectrum and receives the echoes after reflectance on objects. Thus, this technique is an active remote sensing system. In the following chapters, the basic principles of radar remote sensing are described briefly. For further insight into this topic, the studies of Lillesand et al. (2004), Elachi (1988), Woodhouse (2006) and Sabins (1978) give a comprehensive overview in radar remote sensing.

3.5.1 Principles of Side-looking Radar (SLR) Remote Sensing

Wave-lengths of the electromagnetic spectra for radar range from 1 mm to 1m. Most common bands are listed in Table 4.

Table 4: Radar Band Designations

Source: modified from http://rst.gsfc.nasa.gov/Sect8/Sect8_1.html (20.05.2008)

Band	Frequency	Wavelength in cm
K	26,500-18,500 MHz	1.1-1.7 cm
X	12,500-8,000 MHz	2.4-3.8 cm
C	8,000-4,000 MHz	3.8-7.5 cm
L	2,000-1,000 MHz	15.0-30.0 cm
P	1,000- 300 MHz	30.0-100.0 cm

Spaceborne radar systems for remote sensing are side-looking antennas (side-looking radar) that transmit microwaves in short pulses. The flight-direction of a satellite is called azimuth-direction and the direction of the orthogonal looking radar-sensor is called range-direction. The transmitted pulses move radially away from the antenna towards the earth's ground and are either scattered away or

reflected on an object backwards into the direction of the antenna. These backscattered signals are registered relating to their phase, intensity and return time. Basing on that return time, the range, or distance to the objects is calculated. (Lillesand et al. 2004)

The resolution of a radar system depends on the slant range and the corresponding ground range resolution and the azimuth resolution:

- The slant range image is the display of the measured distance between objects and sensor. After terrain correction of every measured point in the data you get the corrected ground range image.

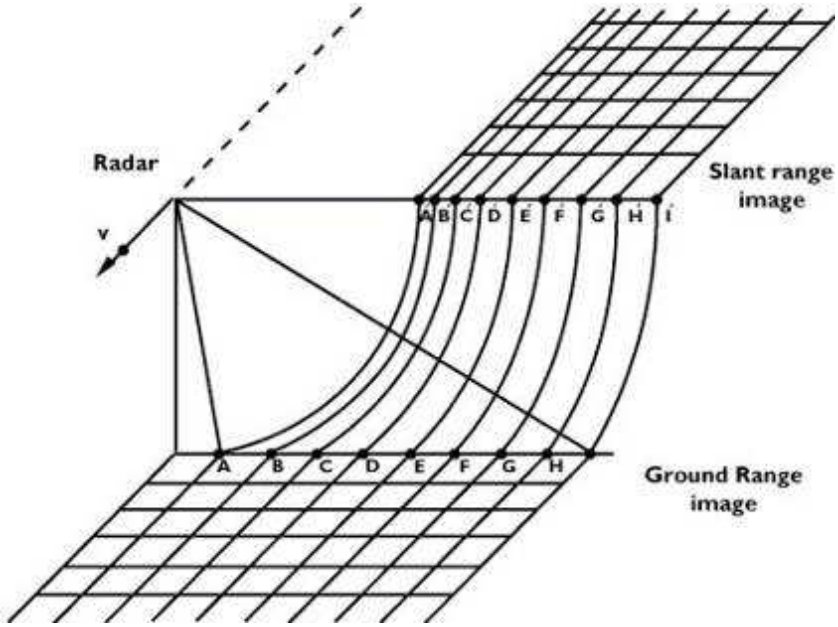

Figure 5: Difference image from slant range to terrain corrected ground range

Source:http://earth.esa.int/applications/data_util/SARDOCS/spaceborne/Radar_Courses/Radar_Course_III/slant_range_ground_range.htm (05.04.2008)

- Through to the movement of the radar system, the azimuth resolution depends on the ending points of the bidirectional scans and the beamwidth of the antenna.

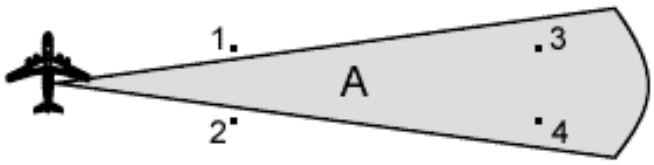

Figure 6: Example of azimuth resolution. For example, in the figure objects 1 and 2 can be determined, whereas objects 3 and 4 come out as single objects.

Source: http://hosting.soonet.ca/eliris/remotesensing/bl130lec13.html (05.04.2008)

The resulting pixel-size of the azimuth-resolution and the ground range is called pixel-spacing, which should not be mistaken for geometrical resolution. Thus, pixel-spacing gives the space between two pixels in an image and the geometrical resolution describes the distance that is necessary to distinguish between two objects in an image. (Schneiderhan 2006)

3.5.2 Real Aperture Radar

For so-called real aperture radar antennas, which are antennas that send out signals at one end and receive signals at the other end, there are physical limitations that can be described through the equation:

$$\delta_x = \lambda_{el} \frac{L_{SOB}}{D_{RAR}} [m]$$

The distance between the satellite and the object is named L_{SOB} and the resolution in the azimuth-direction is named δ_x .The wave-length of the radar system is described by λ_{el}, and D_{RAR} is the length of the radar antenna (Elachi 1988). The resulting limitation of this aperture arises from the length of the antenna if you want to implement it on a space platform, for example. If you solve the equation with the aim of very high-resolution for radar satellite (see Chapter 3.6), you take average values like an azimuth-resolution of 2 meters and an average distance from the antenna and object of 540.000 m and a wave-length of 0,031 m, like the TSX. Then, the corresponding antenna-length would be 8.370 meter. It is obvious that such an antenna is quite impossible to implement in space. That is why this problem is taken care of in synthetic aperture radar (SAR) systems.

3.5.3 Synthetic Aperture Radar (SAR) systems

The function of an SAR system is called synthetic due to the capability to synthesize the effect of a very long antenna. The motion of the radar sensor is used to convert one short antenna into an array of aligned antennas. Due to mathematical models, these successive positions and the recorded data of the moving antenna are processed and linked together. Thus, a very long antenna can be synthesized with an actually very short transmitter and receiver.

Antennas as long as several kilometres can be synthesized with spaceborne SAR systems because points on the ground at near range are viewed by proportionally fewer antenna elements than those at far range. Thus, the effective antenna length increases with range and this results in essentially constant azimuth-resolution irrespective of range. (Elachi 1988; Lillesand et al. 2004) For more detailed information about the mathematical approaches behind the SAR see Elachi (1988).

3.5.4 Geometric Effects of SLR

In order to understand the imagery of the side-looking radar, it is essential to know how the terrain affects the geometry of those images. In Figure 8, the effects are displayed exemplarily for foreshortening, layover and shadow.

The radar sensor measures the time-delay between each radar pulse and its reception (see Chapter 3.5.1). If the radar pulse reflects off the mountaintop first, the mountaintop (Figure 8-A) will be suggested as being closer than the foot of the mountain. This phenomenon is known as foreshortening.

Mostly in near range, a steeper incident angel can cause a layover effect (Figure 8-B), which results in the loss of one side of the mountain in the radar image. This happens when the point of intersection of the perpendicular with the slope line is above the object.

Other usual characteristics of most radar images are shadows that get produced mainly on the leeward sides of high objects as a consequence of the absence of radar illumination (Figure 8-C). These effects happen mainly with large incidence angle illumination. On the other hand, shadows enhance the lineaments, joints, and faults by accenting changes in feature orientation. (Agence spatiale canadienne 1996; Lillesand et al. 2004)

3.5.5 Speckle and Backscatter Effects

Mostly all radar images come out with some degree of a "salt and pepper" texture what is commonly known as radar speckle. This is caused by random interference that occurs within each resolution cell from multiple scattering returns. That means, after interacting with objects on the earth's surface, backscattered waves are not longer in the phase, which produces light and dark pixels in the radar image. Therefore, it can be very challenging to interpret images with a high content of speckle, but on the other hand, speckles carry information about the ground surface and targets. Several filter techniques can enhance the image by reducing speckle and enhancing the contrast for the interpreter, i.e. see in Figure 7 a part of Amnabak before and after modification with a Lee-filter.

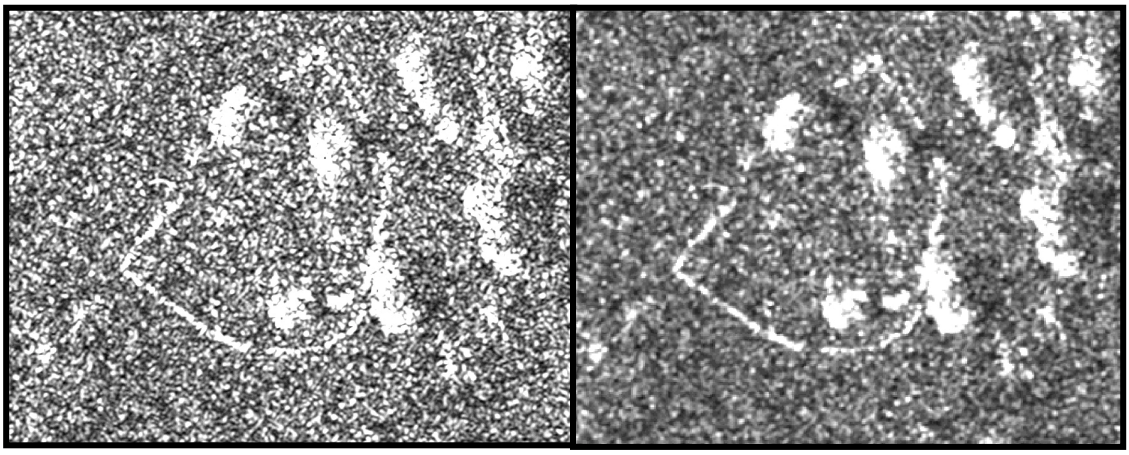

Figure 7: Detailed image of trees and a fence area in a TerraSAR-X scene of Amnabak. Left image shows high content of speckle, right image with reduced speckle after lee-filtering.

The polarisation and the wavelength of the transmitted waves are important parameters for detection of features on the ground in respect to the amount of speckle or recognisability in the resulting radar image. In turn, on the ground the materials and geometry of the target objects mainly influence the backscattering effects that are again interconnected with polarisation and wavelength. In contrast to images received from optical sensors, that contain the information about the absorption, reflexion, or transmission of the sun light in surface materials according to the chemical composition, radar microwaves are reflected by the earth surface due to physical and electrical properties. The strength of radar backscatter is affected by slope, roughness, vegetation cover and the conductivity

of a target. Further information is given in chapter 5, where the images are interpreted, and in the cited literature. (Albertz 2001; Lillesand et al. 2004; ERDAS 2005)

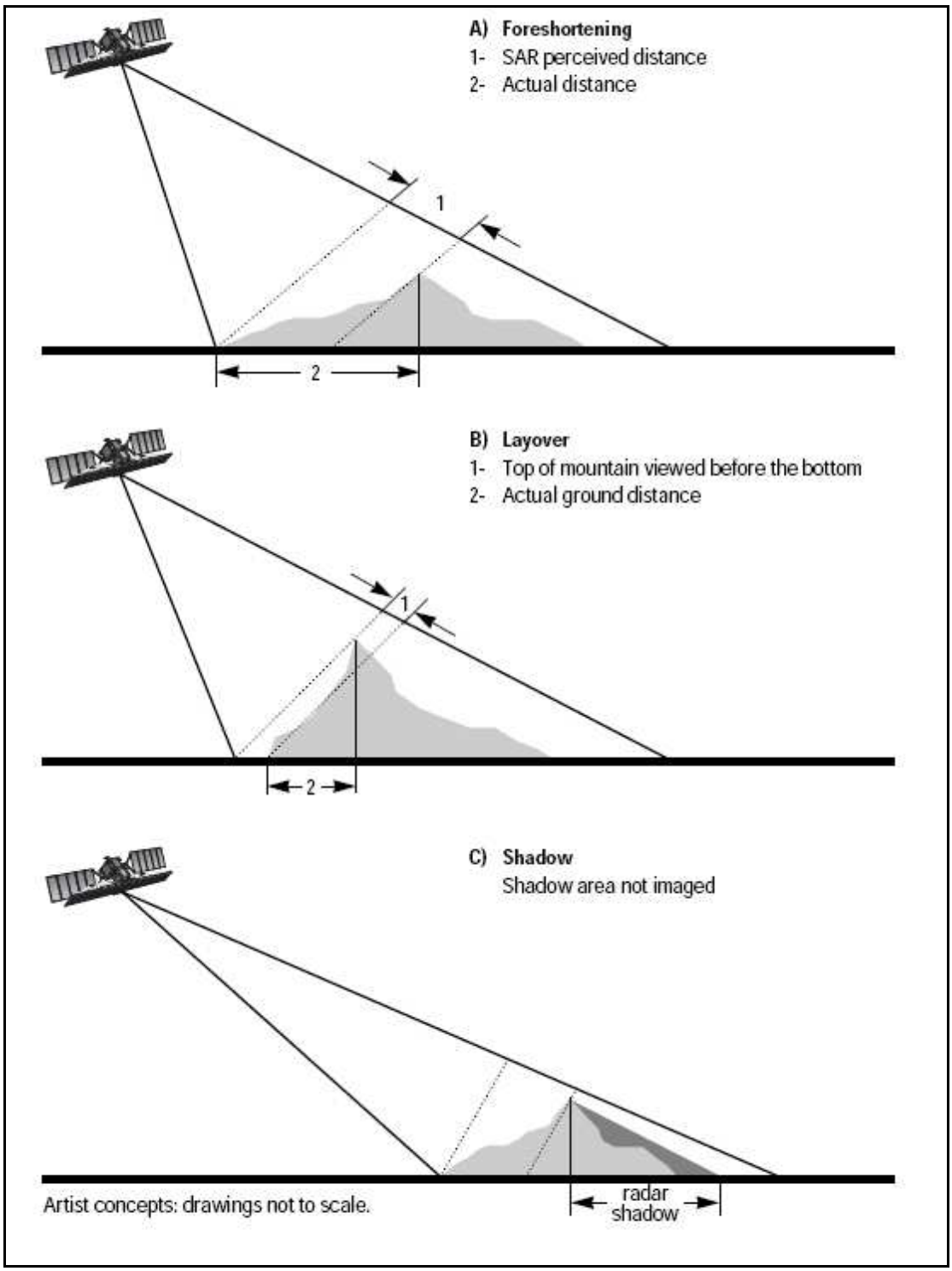

Figure 8: Effects of terrain relief on viewing geometry of Radar Remote Sensing Satellites. Displayed are the effects of A) Foreshortening; B) Layover; C) Shadow.

Source: (Agence spatiale canadienne 1996)

3.6 High Resolution Radar Satellites

Remote sensing satellites using high resolution X-band radar were commonly used for military application only. Since 2007, the German TSX and Italian Cosmo-SkyMed 1 and 2 satellites provide these kinds of data for the scientific community. Several X-band products ranging from 30m to 1m ground resolution are available.

3.6.1 COSMO-SkyMed

The COSMO-SkyMed system is a constellation of four Italian satellites using high-resolution radar to observe the Earth's surface. Cosmo-SkyMed-1 and CosmoSkyMed-2 were launched on June 08th and December 09th, 2007.
The satellites move in a sun-synchronous orbit with an inclination of 97.86° and a repeat cycle of 16 days in single mode. With all four satellites a repeat cycle of 4 days is expected. All satellites are equipped with an X-band (9.6 GHz) synthetic aperture radar (SAR), which can run different modes and provide several data products:

- SPOTLIGHT, allowing SAR images with spot extension of 10x10 km and spatial resolution equal to 1x1 m single look with possible polarisation HH or VV.
- STRIPMAP (HIMAGE), achieving medium-resolution, wide swath imaging, with swath extension of 40 km and spatial resolution of 3x3 m single look and HH or HV or VH or VV for selectable polarisation.
- STRIPMAP (PINGPONG), achieving medium-resolution, medium swath imaging with two radar polarizations selectable among HH, HV, VH and VV, a spatial resolution of 15 meters on a swath of 30 km.
- SCANSAR (WIDE and HUGE region), achieving radar imaging with swath extension selectable from 100x100 km (WIDE REGION) to 200x200 km (HUGE REGION), and a spatial resolution selectable from 30x30 m to 100x100 m. Polarisation can be ordered in HH or HV or VH or VV.

Additional information about orbit, attitude and system parameters is given in Table 5 and can be gathered from the comprehensive handbooks edited by the Italian Space Agency. (Italian Space Agency 2007b, Italian Space Agency 2007a)

Table 5: Orbit, attitude and system parameters of Cosmo-SkyMed

Nominal orbit height at the equator	619.6 km
Orbits / day	14.8125
Revisit time (orbit repeat cycle)	16 days
Inclination	97.86°
Ascending node equatorial crossing time	18:00 (local time)
Attitude steering	”Total Zero Doppler Steering”
Radar carrier frequency	9.6 +/- 0.2 MHz
Radiated RF Peak Power	2 kW
Incidence angle range for stripmap/ Scan-SAR	25° - 50° full performance (20° - 59.5° accessible)
Polarizations	HH, VH, HV, VV
Antenna length	5.7m
Nominal look direction	right
Incidence angle range for spotlight modes	20° – 55° full performance (20°-59.5° accessible)
Pulse Repetition Frequency	2.0 kHz – 6.5 kHz
Range Bandwidth	max 150 MHz (300 MHz experimental)
Radar carrier frequency	9.6 +/- 0.2 MHz
Radiated RF Peak Power	2 kW

3.6.2 TerrraSAR-X

The German radar satellite TerraSAR-X was launched on June 15th, 2007 and is the first earth observation satellite that provides SAR data in X-Band (9,65 GHz). TSX has an inclination of 97.44° and moves along a sun-synchronous orbit with a repetition rate of 11 days. The satellite operates with different acquisition modes and polarisations:

- The ScanSAR mode provides 100 km wide strips with an acquisition length of max. 1650 km at a geometrical resolution of 16 meters
- Stripmap with 30 km wide strips with an acquisition length of max. 1650 km at a geometrical resolution between 3 and 6 meters
- Spotlight mode with 10x10 km or 10x5 km scenes at a varying geometrical resolution of 2 or 1 meters.

Possible polarisations are HH, VV, HV, VH in single or dual mode (except ScanSar, which is only in single polarisation). Additional information[5] about the orbit, attitude and system parameters is given in Table 6.
(CAF 24.02.2008)

[5]For further Information visit: http://www.dlr.de/tsx/documentation/SAR_Basic_Products.pdf

Table 6: Orbit, attitude and system parameters of TSX

Nominal orbit height at the equator	514 km
Orbits / day	15
Revisit time (orbit repeat cycle)	11 days
Inclination	97.44°
Ascending node equatorial crossing time	18:00 ± 0.25 h (local time)
Attitude steering	”Total Zero Doppler Steering”
Radar carrier frequency	9.65 GHz
Radiated RF Peak Power	2 kW
Incidence angle range for stripmap / Scan-SAR	20° – 45° full performance (15°-60° accessible)
Polarizations	HH, VH, HV, VV
Antenna length	4.8 m
Nominal look direction	right
Antenna width	0.7 m
Number of stripmap /ScanSAR elevation beams	12 (full performance range) 27 (access range)
Number of spotlight elevation beams	91 (full performance range) 122 (access range)
Number spotlight azimuth beams	229
Incidence angle range for spotlight modes	20° – 55° full performance(15°-60° accessible)
Pulse Repetition Frequency	2.0 kHz – 6.5 kHz
Range Bandwidth	max 150 MHz (300 MHz experimental)

3.6.3 TerraSAR-X Spotlight Data of Amnabak & Koubigou

The analysis of a refugee or IDP camp with high-resolution X-band data is a very new approach that was mentioned in several works of research literature. For that purpose, the following data shown in Table 7 and

Table 8 were ordered to examine the opportunities of high-resolution radar imagery with TSX.

Table 7: Dataset for TSX Spotlight-mode Image Amnabak

Creation Date:	19.03.2008
Processing Level:	Level 1b
Data product:	Spotlight – spatially enhanced
Interpolation Method:	Cubic Convolution
Map Projection:	Universal Transverse Mercator
Zone Number:	34 North
Datum:	WGS84
Incidence Angle:	49.028 - 49.424
Polarisation:	S (VV)
Imaging Mode::	HS 300MHz (Experimental)
Orbit:	C26-55 (4230) A
Acquisition Date (YYYY-MM-DD)	2008-03-19
Acquisition Time (hh:mm:ss):	16:42:16.99673 – 16:42:17.73862
Orbit direction	Ascending
Ground range resolution	1.033 meter
Azimuth resolution	1.179 meter
Pixel Size:	0.5 meter

Table 8: Dataset for TSX Spotlight-mode Image Koubigou

Creation Date:	03.04.2008
Processing Level:	Level 1b
Data product:	Spotlight – spatially enhanced
Interpolation Method:	Cubic Convolution
Map Projection:	Universal Transverse Mercator
Zone Number:	34 North
Datum:	WGS84
Incidence Angle:	38.800 ..39.413
Polarisation:	S (VV)
Imaging Mode::	HS 300MHz (Experimental)
Orbit:	C25-55 (4063) A
Acquisition Date (YYYY-MM-DD)	2008-04-03
Acquisition Time (hh:mm:ss):	16:41:40.34700 – 16:41:41.09627
Orbit direction	Ascending
Ground range resolution	0.961 meter
Azimuth resolution	1.117 meter
Pixel Size:	0.5 meter

3.6.4 Advantages and Limitations

In general, active radar remote sensing faces the same benefits and limitations as described in chapter 0 for optical VHRS imagery, but apart from that it has the advantage that microwaves can penetrate the atmosphere without the restrictive effects that are involved when working with optical sensors. Radar can “look” through clouds, haze, light rain and smoke with most wavelengths. Also, the

independence from sunlight is another important benefit in contrast to optical remote sensing data. This weather-independent night and day capability makes radar remote sensing a powerful tool for many services, especially when the area of interest is located in a geographical region where atmospheric influences are high, such as the tropics.

By looking on a satellite image derived from optical sensors, the viewer gets an intuitive impression of the recorded area. In contrast, interpreting radar data needs wide knowledge of the characteristics of radar remote sensing and a great expertise in the understanding of the received data in respect to the features on the ground. Further aspects in this context are given in chapter 5.2.

4 Methods for Shelter Extraction

The tested techniques for information and particularly shelter extraction in refugee and IDP sides follow the methods of Giada et al. (2003b), Bjørgo (2000) and the ENVIREF final report (Dalen et al. 2000).
The multi-spectral VHRS imagery (see Chapter 3.4.1) from the refugee camp Amnabak and the IDP site Koubigou were analysed by visual interpretation, pixel-based and object-based classification. The methods were compared due to the accuracy of the results, the temporal effort and the transferability of the methods to each campsite. The analyses were performed with the GIS software ArcGIS 9.2 from ESRI, Definiens Developer 7 from Definiens, and the remote sensing program ERDAS IMAGINE 9.1 from Leica Geosystems Geospatial Imaging.

4.1 Image Preparation and Enhancement

The IKONOS data were already delivered with a geometric correction and ortho-rectification as 1-meter resolution pan-sharpened multi-spectral images from European Space Imaging.
The first steps of the image preparation were producing subsets of each campsite to gain a better overview for visual interpretation and require less calculation time for pixel and object based methods. To present optimal results for the interpretation methods, the satellite images were tested with different techniques in spatial, radiometrical, and spectral enhancement (Chapter 3.4.2). The aim was to reach a visibility of the shelters, which is as precise as possible. For that reason, texture, adaptive and statistical filtering was proved. Complex atmospheric corrections were unnecessary since there was no cloud cover and only a slight impact of haze in both data sets.

4.2 Visual Interpretation

Satellite imagery shows a detailed record of a one-time moment on the earth surface. The viewer detects objects with different shape and size and identifies these through his individual perception and expertise. Photographs from the area

of interest and shared knowledge from others can be a useful support for the interpreter. Success varies due to the training and experience of the interpreter and surely by reason of the quality of the image, regarding radiometric and geometric distortion. A common understanding of the phenomena being observed is as necessary as a basic knowledge about the geographic region. The interpreter has to be familiar with perspectives from overhead, using wavelength outside the visible spectrum and the display of the earth's surface in different scales and resolutions. Most applications follow the characteristics and variations of:

- Shape, like the general form or outline of an object
- Size, regarding the image scale and resolution
- Pattern, spatial arrangement of natural and constructed subjects
- Tone, like the relative brightness or colour; without variations of tone, shapes, patterns, and textures can not be distinguished
- Texture, the smoothness and coarseness in the image due to the change in frequency of tone
- Shadows, aid to get a better impression of the profile of an object (the sun's azimuth and angle should be written in the image's product data sheet)
- Site, the geographical information and the association with the features
- Resolution, the limits for interpretation of small objects due to their visibility and contrast in the image
- Time, temporal aspects like changes in the environment from day to inter-annual variability, which is only possible when a time series is available.

It has to be mentioned that there is no concrete recipe to conduct a visual interpretation. The strategy to approach the interpretation differs concerning the function of the available data and background information (Lillesand et al. 2004)

4.2.1 Description of Amnabak

The refugee camp extents from the images' southeast to its northeast and the village of Amnabak is located in the west. Dry riverbeds called *wadis* run through

the entire area from south to north. Sparse vegetation like several trees, bushes and grassland are dotted sideways the stream's course. One main road, which is north-to-south-oriented, leads through the village. Two smaller tracks turn into the camp area, where they split up and fade on into numerous field- and footpaths. The camp's narrow structure is very inhomogeneous due to the pattern of dwellings. There is no logical positioning recognizable like structures of rows or blocks. Most of the shelters have a high reflectance in all visible bands and the NIR. Some shelters stand alone but mostly in agglomerations surrounded by fences. Within a short distance from the camp, larger buildings can be detected in an adjacent area. They can be interpreted as facilities of humanitarian relief organisations.

4.2.2 Description of Koubigou

From the southwest along a major road to the north, the IDP site spreads into the centre of the images' subset. In the northwest, the village of Koubigou is located in a block-like ordered shape. Also, the IDP camp's centre looks like well-arranged quarters, which differ just a little in shape and extent. Apart from the centre, the northern and southern ending parts of the camp are more chaotic with a higher density of dwellings. Most of the shelters are in fenced agglomerations, whereas the number of shelters can vary from three up to over twenty - increasing from the centre part outwards to the northeast and southwestern part. Both, village and IDP site, are crisscrossed by several streets and fieldpaths. Between the two settlements, some bigger buildings are dotted in an open space. In the south of the camp, a hilly train with spotted tree or bush vegetation adjoins. There are segments of fields around the camp and village with scattered trees and bushes within the village and along two dry rivulets in the east.

4.2.3 Visual Interpretation Technique

After the general and oblique interpretation of both campsites and in respect to the UNHCR document *Step-by-Step Guide Mapping a Refugee Camp* (UNHCR - Population Data Unit 2005), it was decided that only shelter and infrastructure were expedient to extract. Thus, the following techniques have been applied.

- The feature extraction was done in ArcMap which is part of the ArcGIS. Shelters were stored as points and streets were stored as polylines and labelled with three categories: main roads, roads, and footpaths.

- Grid-by-Grid technique. The subset, which was produced for Amnabak, covers 2.86 square km, the one for Koubigou covers 3.94 square km. An image that shows many small features, which are in an unsystematic alignment, accurate counting poses big challenges to the interpreter. Thus, a grid with 100x100 meter cells was added to the subsets of both images to count and extract the shelters grid-by-grid without confusion. The grid was constructed in ArcGIS and got prepared with fixed geographical coordinates for accurate proximal statistical evaluation of the different shelter extraction methods.

- Image enhancement was accomplished with ERDAS IMAGINE 9.0. It was found out that the best support for the visual shelter extraction was given by the first principal component analysis (PCA) for higher contrast to the surrounding features and distinction of light bluish haze effects in both images.

- To highlight various features or phenomena, several band-combinations in red green and blue were applied i.e. NIR-RED-GREEN, RED-NDVI-BLUE, RED-NIR-GREEN etc.

- The sun's azimuth is in both scenes around 140° with an angle of approximately 65°. That fact together with zero cloud cover should create shadows besides the northeastern edges of feature like tents, huts, or other shelters.
-

Figure 9: Zoom into true colour image with red, green, and blue band combination and beneath a grey scale image out of the first principal component.

- For separation of huts and trees, the near infrared channel (NIR) was used in different band combinations. Furthermore, a natural differenced vegetation index (NDVI) was applied for identifying healthy vegetation. It divides the difference of the NIR and RED channel by the sum of the two bands. Chlorophylls, the primary photosynthetic pigments in green plants absorb light primarily from the red and blue range of the electromagnetic spectra. Infrared is reflected to a higher extent that is why NDVI tends to increase in green leaf biomass. Surfaces out of rock and bare soil display in values near zero. (Lillesand et al. 2004)

$$NDVI = \frac{(NIR - RED)}{(NIR + RED)}$$

- Identification of shelters and surrounding features of the two testing sites Amnabak and Koubigou was supported by an intensive internet research for photographs and articles describing the actual situation in such locations or comparable refugee or IDP camps.

- Google earth was used to get an overview and a general impression of similar campsites and of the surrounding environment.

- Measurements and approximations of surface elevation as well as terrain slope were taken from the corresponding SRTM-data (Shuttle Radar Topographic Mission), which contains information about the height,

4.3 Results from Visual Interpretation

4.3.1 Shelters

The shelters that were extracted in both sites have a very high reflectance in all visible bands and an almost rectangular shape. The size varies from 8 – 20 square meters whereas only the centre part of the white rooftop sheet reflects in constant bright spectra. Shadows appearing adjacent to the northwestern edges to the dwellings were used for validation that the objects have a vertical height and are not flat, i.e. a plastic cover on the ground for sitting. Beside the white shelters in Amnabak, various unidentifiable dark, round and rectangular features are placed just some meters away within the fenced agglomerations of dwellings. It was not possible to generate reliable results without any groundtruthing. Due to this, pictures from comparable camps were used for identification. A photograph of the similar UNHCR camp Iridimi (Figure 10) shows an excellent example of the situation on the ground. The white appearing features in the imagery were identified as makeshift shelters with plastic sheets from UNHCR, which were tied to the roof in order to provide adequate protection against rain, wind and sun. Next to that, there are open areas with the same size like the dwellings, which are likely to be used for livestock or other property.

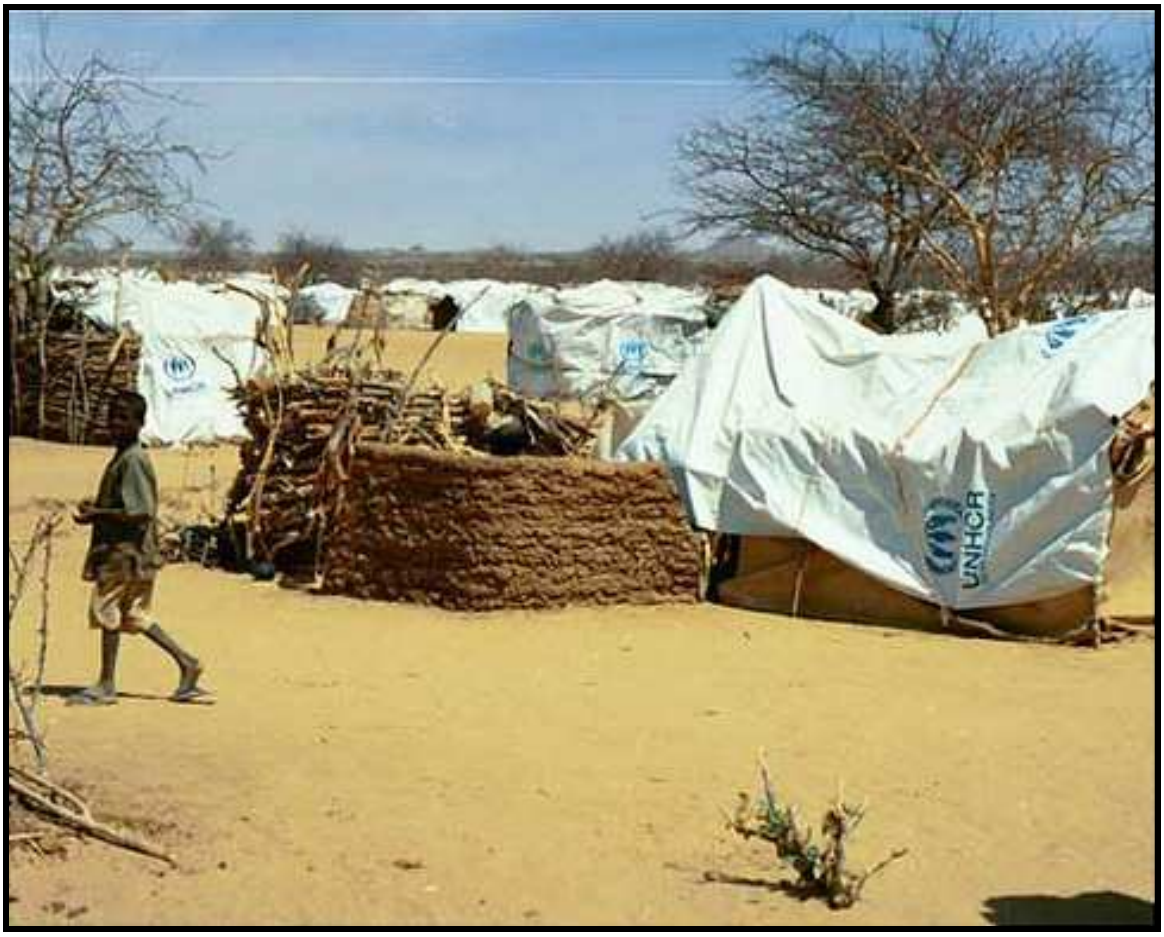

Figure 10: White shelter with a fenced open area built from local materials. Source:http://www.ushmm.org/conscience/alert/darfur/staring_genocide_in_the_face/

The situation in Koubigou is similar to Amnabak regarding unidentifiable features beside the white shelters. It was also not possible to definitely classify them as huts, stables or other anything similar. Further estimates from visual interpretation are given in the interpretation of the radar remote sensed TSX Spotlight images in chapter 5.

2158 shelters in Amnabak (an example of the resulting map is shown in Figure 11) and 500 shelters in Koubigou were clearly identified within 2.5 and 1.5 hours, respectively and it took 40 and 30 minutes to extract the locations' infrastructure. All results are listed in Table 9 and Table 10.

Table 9: Results from the visual interpretation of Amnabak

Extracted features for Amnabak	Results in time and number
Required time for infrastructure mapping	40min
Required time for shelter mapping	2.5 h
Number of white shelters	2158

Table 10: Results from the visual interpretation of Koubigou

Extracted features for Koubigou	Results in time and number
Required time for infrastructure mapping	30min
Required time for shelter mapping	1.5 h
Number of white shelters	500

4.3.2 Infrastructure

As for the locations' infrastructure, streets were mapped with a modified definition key of the Step-by-Step guide Mapping a Refugee Camp UNHCR - Population Data Unit (PGDS) 2005.

Three different types of streets were identified (see Figure 11):

- Main roads are large roads, which can accommodate vehicular traffic and are the main thoroughfares to the camps.
- Roads are smaller tracks, which are not frequently used and are mainly passable for 4-wheel-drives.
- Footpaths are trails within the camp, which are too narrow for vehicles.

The streets in Amnabak are not always clearly distinguishable from the drainage tracks and *wadis*. It was presumed that both are used as transport infrastructure in dry season. The streets in Koubigou are easier to map as a result of the block-like arrangement of the site.

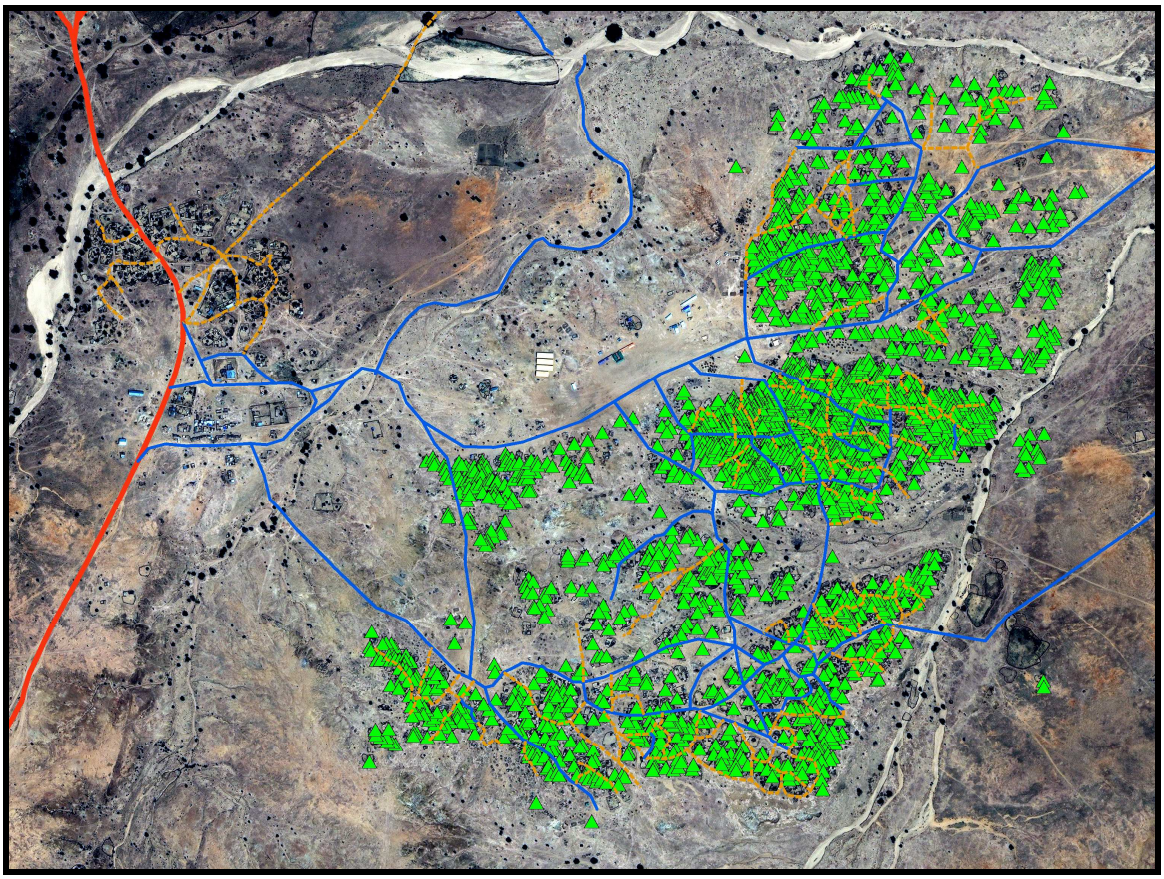

Figure 11: Visually mapped features in Amnabak. Streets and white shelters were extracted and labelled in red for main roads, in blue for roads, in dashed orange for footpath and with green triangles for shelters

4.3.3 Environmental Aspects

Vegetation cover in the two camps and their proximity differs significantly. An NDVI was made from both full extended scenes to examine changes in land cover concerning the surrounding environment and within the sites with different scales.
In a scale of 1:50.000 the refugee camp Amnabak sets apart from its natural environment and gets displayed as a dark spot because of little backscatter in the NIR. By showing the image in a scale of 1:2.500, some sparse vegetation along the wadis and very few spots inside the camp become visible. When analyzing the image in natural colour composition, some of the trails and roads, which run from west to east into the direction to the wadi, look as if they were formed by fluvial dynamics. That is most likely because of the lack in sufficient vegetation cover due to deforestation for firewood collection and the need for fodder of the people's livestock. The difference in height for the campsite and the nearby wadi was checked with SRTM-data and amounts about 5-10 Meters. Consequently, due to the difference in altitude erosion during rainfalls becomes a possible matter of soil degradation and also a hazard for refugees because shelters are not positioned on a solid underground.
The IDP camp Koubigou has brighter reflections in the NIR band as Amnabak. Examined at a scale factor of 1:50.000, it does not differ much from its natural environment but can still be identified. So it seems that the surrounding vegetation is not dramatically influenced by the camp's inhabitants, yet. In a scale of 1:2.500, the NIR are shows high differences in vegetation of places in the north and south of the camp as well as in between camp and village. These places appear dark in the NDVI and are interpreted as spots of high activity of people or transportation. The environment of the neighbouring village is in a better condition, probably as a reason of less population.

4.4 Pixel-based Information Extraction

Giada et al. (2003b) tested the unsupervised and supervised classification for information extraction of refugee camps in his approach. For this study, an additional threshold-classification was added to get a wider range of information extraction techniques.

Pixel-based classification, also known as multi-spectral classification, uses the values of single pixels in an image. This process is also called spectral pattern recognition, where spectral attributes on a numerical basis are used. Context information like spatial characteristics of the surrounding pixel is not taken into account. The classes for classification differ in specific combinations of the digital numbers from each recorded spectral band. These values accord with the typical reflection values of the classified features. (Lillesand et al. 2004)

The pixel-based information extraction was performed by the remote sensing software ERDAS IMAGINE 9.1. The accuracy assessment of all methods was completed in ArcGIS. Regarding to the missing field data, the most precise information was available from the visual interpretation, which was assumed as the ground truth data for the accuracy assessment.

4.4.1 Supervised Classification

In this type of classification technique, the image analyst controls the process of the specific imaging software. Thus, categorisation of pixel values and computer algorithms is supervised to extract various land cover classes. (Lillesand et al. 2004)

The pixel values for a specified number of bands are selected from areas in the scene that are a priori identified. These chosen values, also known as training areas, are representative for the features or materials that are wanted to be classified. Common classes can be for example sand, streets, water, grasslands, scrub brush, or various tree species and so on. The training areas are used to develop a numerical interpretation key that contains the spectral attributes for the wanted classes. By using the interpretation key, each pixel in the image is compared numerically to each created category and is then classified into the most likely group by selected statistical methods. Most common statistical methods are detailed in Lillesand et al. (2004). As for very high-resolution images, it is known that pixel-based classification can yield high speckle-like results. The unwanted classification of numerous small objects in the background can be solved with image processing techniques.

The first step during the supervised classification was the consideration of meaningful and possible classes. Therefore, visual interpretation and Giada's approach (2003b) were used. Goetz et al. (2003) used the supervised classification for extracting vegetation cover from IKONOS images. That technique was partially used for the current method in this thesis. Spectral signatures were taken to create similar classes, just as Giada did (2003b), who uses the classes tents, roads, bare soil and buildings. For this thesis these classes were extended and modified to:

- *white shelters*, to allow the comparison with other extraction techniques, which is the main aim of the thesis
- *living structures* that represent the materials, which are detected around the white shelters for recognizing misclassified shelters in a first visual assessment
- *trees* and *sparse* vegetation, which are part of natural resources in the region for fire wood and fodder
- *streets* and *wadis,* which are used as streets, therefore, being part of the infrastructure
- *soil* and *bare soil* to estimate the contingent of erosion
- *buildings* to examine the differences in the structure of villages and campsites

After several tests it was decided to merge the class streets and wadis into the class bare soil because of the similar spectral reflectance and the assumption that the seasonal water flow in wadis, eroded most of the soil out of the river bed.
Subsequent to defining the concrete classes, the classification was tested with ERDAS IMAGINEs parametric and non-parametric decision rules. The best result regarding the white shelters was set with a non-parametric decision rule that does not use statistical rules like Mahalanobis Distance or Maximum Likelihood. For other classes, a more precise classification can be obtained with parametric rules, which could be used in further research.
The extracted class white shelters was separated from the resulted raster file and transformed into a vector file in ArcGIS. The measured size from the visual

interpretation of white shelters is between 8-20 square meters (Chapter 4.3.1), but mostly the centre part of the white plastic sheet reflects in constant spectra and for that reason, an area threshold was set to delete the speckle-like classifications that were below 2 square meters.
For an accurate accuracy assessment, the comparison with the results of the visual interpretation was applied.

4.4.2 Unsupervised Classification

In an unsupervised classification, the purpose is to group multi-spectral response patterns into discrete clusters that are statistically separable. Unsupervised classification methods do not use any training area for the categorization. All pixels are classified to the cluster, which each pixel is most likely to belong to. The resulting image is produced in black and white or in colours assigned to each cluster. This must be interpreted by the analyst regarding to what the colour patterns mean in terms of classes or what they actually present in the real world scene. The patterns do not necessarily correspond to meaningful classes of features as it is defined in a supervised classification but rather to grouped pixels that have the similar spectral characteristics. (Lillesand et al. 2004)
An unsupervised classification performed by ERDAS IMAGINE uses the ISODATA (Iterative Self-Organizing Data Analysis Technique) algorithm. ISODATA is iterative by repeatedly performing an entire classification and recalculating statistics. Furthermore, it self-organizes the location of the clusters that are inherent in the data and uses the minimum spectral distance formula to form the clusters. It starts with an arbitrary cluster means or with means of an existing signature set. Each time the clustering repeats, the means of these clusters are shifted, and then the new cluster means are used for the following iteration.
The ISODATA algorithm redoes the clustering of an image until a maximum number of iterations have been calculated, or a maximum percentage of unvaried pixels has been reached between two iterations. (ERDAS 2005)
The interpreter can modify the process within the following parameters:

- The number of the out-coming classes
- The amount of maximum iterations

- The maximum amount of unvaried pixels between two iterations through a convergence interval error margin

The aim of this unsupervised classification was to mine classes that are like the classified features that were identified during the visual interpretation. Anyway, it was assumed that only features with homogenous spectral attributes could be extracted due to the functionality of the ISODATA algorithm. Giada et al. (2003b) approach for information extraction in refugee camps focused on shelters that appear mainly in the same brightness. After testing the unsupervised classification, it was also decided to follow Giada's procedure in consequence of the unfeasibility to gain more than the shelter class. Classifications were applied with 10 up to 20 classes. With the altering of classes, the ISODATA algorithm increased the differentiation of the amount of similar spectral values in each class. Finally, the class that represented the white shelters most precisely was exported into a vector file and added into a geographical information system (GIS) for further evaluation. The amount of maximum iterations was set on the highest value to assure a complete calculation to the convergence interval error margin, which was left unmodified with 95 % for all classifications. For Amnabak, 16 classes were calculated and for Koubigou 20.

4.4.3 Threshold Classification

Thresholding is generally used for image segmentation of a grey-level image into two classes. The histogram of an image is examined due to the value of the pixels in brightness in a spectral band and then, a threshold is set to separate the image into a class that lays above this certain threshold and into another one that is beneath it. The result is a binary mask, where usually one class gets the value 0 and the other one the value 1. (Lillesand et al. 2004)

This technique was used to separate the white shelters in Amnabak and Koubigou from the background. The process tree for the threshold performance was constructed in the ERDAS IMAGE Knowledge Engineer. Instead of using just one threshold for grey-level image segmentation, the approach was enhanced with thresholds for all bands in the image. For that, the spectral profile of 50 white shelters was taken in both campsites each. The spectral minimum and maximum

values of the samples were examined for both camps (see Figure 12) and then taken into thresholds for each band in order to get a high differentiation to all other features in the images. Hence, the wanted output was limited with an upper and lower margin. All pixel values within this range of the approached thresholds received the value 1, any other values out of the range were considered not to be a shelter and were given the value 0. The resulting binary mask was transferred into a GIS and all features with value 1 were converted into a point shapefiles for subsequent statistical analysis and the accuracy assessment.

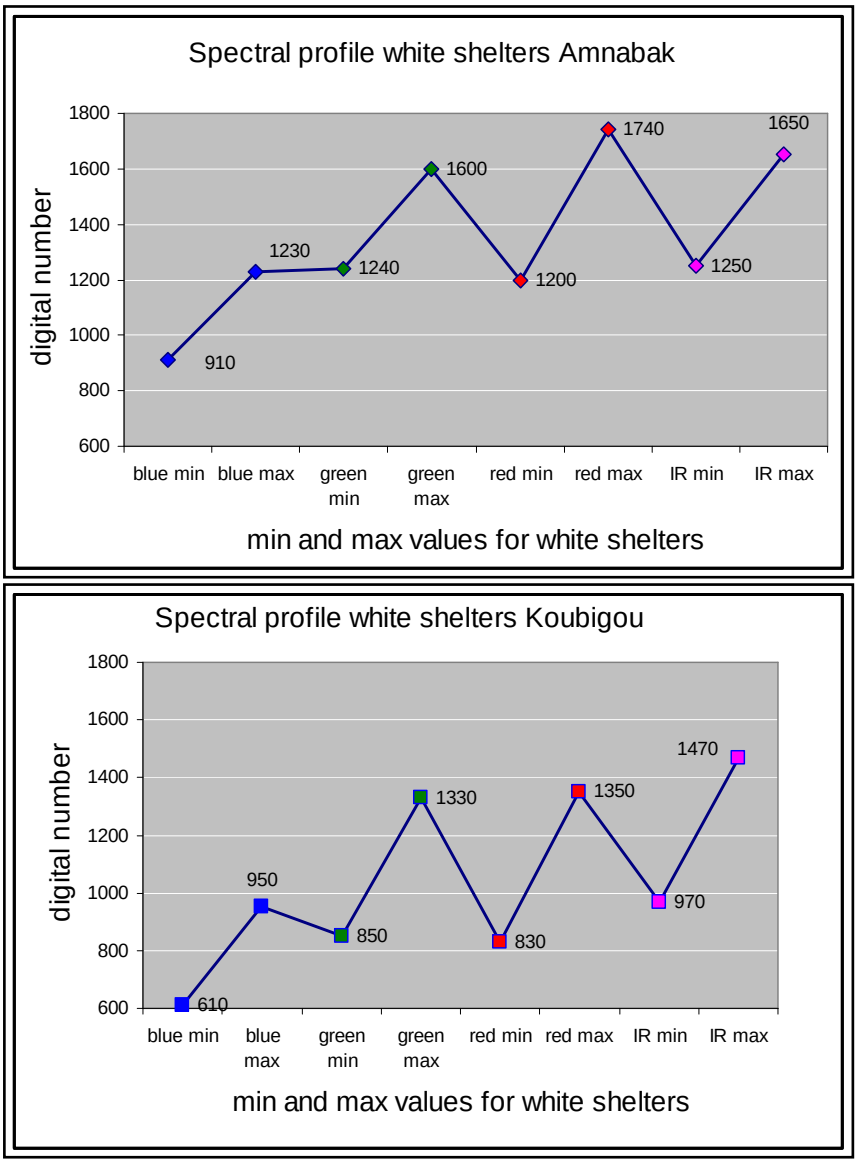

Figure 12: Spectral profile with min and max values of white shelters in Amnabak and Koubigou for threshold classification.

4.5 Results from pixel-based Information Extraction

The outcomes of the pixel-based methods were imported into a GIS, incl. a proper geo-database. After supplementary preparations, the results were validated via accuracy assessment.

4.5.1 GIS based Preparations for further Analysis

Pixel-based classification results in raster data that can be transformed into polygon vector files for adequate postprocessing. Each pixel-based classification method was analysed in respect to size, correct geographical positions and extraordinary conglomerations of the extracted features.

For Koubigou the following preparations were made:

- Due to the very high reflectance of the streets in the southwestern part of the Koubigou site, the ISODATA algorithm of the unsupervised classification method wrongly classified numerous pixels as white shelters. To solve these misclassified features, a buffer of six meters was set along the extracted main streets to eliminate wrongly classified shelters, where no real shelters were examined.

For Amnabak and Koubigou the following preparations were made:

- The measured size from the visual interpretation for white shelters is between 8-20 square meters (Chapter 4.3.1), but mostly the centre part of the white roof reflects in constant spectra that can be used for pixel-based classification techniques. After high-lightening all features below one square meter, it was decided to set an area threshold to delete the speckle-like classifications that were below 1 square meter and above twenty meters.
- The grid for the statistical analysis that was added over both images was adjusted to the relevant area over the campsites. All features that were outside of that area were selected and sorted out.

- Extracted polygons of the class shelter were automatically converted into point-vectors to prevent a duplex counting in the relevant grids because of overlapping of polygons in neighbouring grids.
- Results of each method were counted automatically grid-by-grid with the free ArcGIS extension Hawth´s Analysis Tools.

4.5.2 Outcomes of Pixel-based Classifications

The different classification methods presented very interesting results for both images. For Amnabak, the threshold classification yields 2372 shelters whereas the unsupervised classification carries out 1987, and the supervised 1978. That is a disparity of 394 shelters. With a grid-by-grid counting for each classification method, all results were compared to the reference data. The correctly classified shelters are between 1931 and 1942 shelters, which show a good identifiability for Amnabak (Table 11). The numbers yielded from Koubigou (Table 12) differ from 604 for the supervised classification, 877 for the unsupervised, and 481 for the threshold classification. That makes a difference of 396 shelters of the applied classifications in Koubigou, which is similar to the results in Amnabak. The correct numbers of shelters for Koubigou are between 425 for the supervised, 388 for threshold, and 354 for the unsupervised classification. Furthermore, the difference of correctly identified shelters in Koubigou shows with the number of 71 a bigger variety than in Amnabak with the difference of 11. To point out advanced interconnections between the identified shelters, the correctly identified shelters and the reference data, an accuracy assessment was calculated in the following chapter 4.5.3. An explicit discussion on the results can be found in Chapter 6.1.

Table 11: Identified shelters and correctly identified shelters in the image Amnabak

Classification methods	Identified Shelters	Correctly identified shelters
Supervised	1978	1941
Unsupervised	1987	1931
Threshold	2372	1942

Table 12: Identified shelters and correctly identified shelters in the image Koubigou

Classification methods	Identified Shelters	Correctly identified shelters
Supervised	604	425
Unsupervised	877	354
Threshold	481	388

The correctly identified shelters for both images were figured out visually with a GIS-based comparison of the classified features with the reference data from visual interpretation. This was achieved grid-by-grid for all the 121 grids cells in the GIS of Amnabak and for all the 81 grids in the GIS of Koubigou. The technique is illustrated in Figure 13.

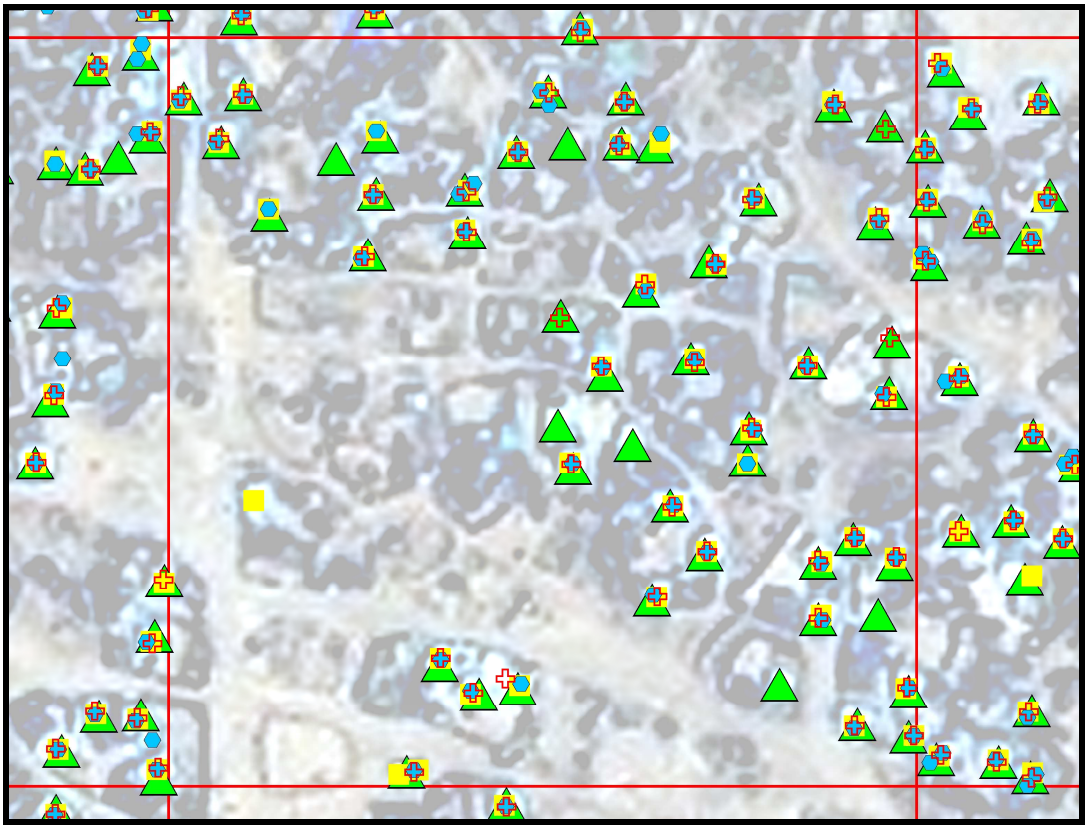

Figure 13: Grid-by-Grid counting for each classification method was done visually for each grid (red lines) in both images. Green triangles represent the reference data that was carried out visually. Yellow quarters are the extracted features from the unsupervised classification, blue dots from threshold, and red crosses from supervised classification. Every sign was compared to the reference data and the amount of correct hits was typed into a corresponding attribute table.

4.5.3 Accuracy Assessment

To ensure an efficient accuracy assessment throughout the pixel-based methods, the results from the visual interpretation were used for the ground truth reference data following Giada et al. (2003b) and Lang et al. (2006). Usually, the ground truth is collected in situ during fieldwork. Due to the circumstances of the general crisis situation in the relevant region, no other data and information was available. The accuracy assessment was performed according to Congalton (1991), who pointed out any necessary considerations and available techniques for a correct validation of achieved classifications in remote sensing. Hence, the user's and the producer's accuracy as well as the all-over accuracy were calculated for all pixel-based methods. All these calculations describe particular characteristics of an applied classification technique and are represented in an error matrix.

- The *producer's accuracy* describes the probability to which the reference data is correctly classified. The total number of a correct classified feature derived from an applied method is divided by the total number of the reference data. That shows the producer how well a specific section can be classified.

- On the other hand, the *user's accuracy* shows the probability to which a classified feature on an image represents the desired category in reality. Therefore, the total number of correctly classified features is divided by the total number of features in this class.

- The *overall accuracy* proves the probability to which a category is correctly classified. The total number of correctly classified shelters is divided by the sum of the correctly and wrongly classified shelters as well as the missing shelters. For that application, we set up the class non-shelters out of the group of wrongly classified shelters.

4.5.4 Exemplary Calculation for Supervised Classification Amnabak

The following accuracy assessment is shown exemplarily for all the different kinds of statistics that were calculated. The example is based on the supervised classification of Amnabak. At first, an error matrix (Table 4) is set up and thereupon the accuracy assessment (Table 14) is produced on the recommendation of Congalton (1991)

Table 13: The error-matrix for the supervised classification of Amnabak

Visual reference data				
Classified data		Shelter	Non-shelter	**Σ**
	Shelter	1941	37	1978
	Non-shelter	217	0	217
	Σ	2158	37	2195

Table 14: Exemplary accuracy assessment based on the supervised classification of Amnabak

User's accuracy = Correctly identified shelters / All identified shelters * 100 User's accuracy = 1941 / 1978 * 100 **User's accuracy = 98.13 %**
Producer's accuracy = Correctly identified shelters / Visual reference data * 100 Producer's accuracy = 1941 / 2158 * 100 **Producer's accuracy = 89.94 %**
Overall accuracy = Correctly classified shelters / (All identified shelters + missing shelters)*100 Overall accuracy = 1941 / (1941 + 37 + 217) * 100 **Overall accuracy = 88.43 %**

4.5.5 Comparison of Pixel-based Methods

The results for all pixel-based techniques are listed in Table 15 and Table 16.
The first column shows all results for the pixel-based classifications that were counted automatically (Chapter 4.5.1) as well as the visually interpreted reference data. In the second column, correctly identified shelters are presented, validated visually grid-by-grid. The GIS-based technique underlying this process is shown in Figure 13 in detail. In contrast to commonly used methods (see chapter 1.3), which entail a particular rate of uncertainty, in this approach no extrapolations were made regarding an enumeration of successful classified shelters.
The numbers of accuracy assessment for the user's accuracy, producer's accuracy and overall accuracy were achieved as shown in the exemplary calculation for supervised classification Amnabak in Chapter 4.5.4, following the adjusted guidelines from Congalton (1991).

Table 15: Statistics for pixel-based methods Amnabak

Classification methods	Identified Shelters	Correctly identified shelters	Users accuracy	Producers accuracy	Overall accuracy
Visual (reference data)	2158	--	--	--	--
Supervised	1978	1941	98.13 %	89.94 %	88.43 %
Unsupervised	1987	1931	97.18 %	89.48 %	87.22 %
Threshold	2372	1942	89.99 %	81.87 %	75.04 %

Table 16: Statistics for pixel-based methods Koubigou

Classification methods	Identified Shelters	Correctly identified shelters	Users accuracy	Producers accuracy	Overall accuracy
Visual (reference data)	500	--	--	--	--
Supervised	604	425	85.00%	70.36%	62.59 %
Unsupervised	877	354	70.80%	40.36%	34.60 %
Threshold	481	388	77.60%	81.67%	65.43 %

4.6 Object-Based Analysis

Classifications on remotely sensed images are traditionally based on the multi-dimensional feature space of measured reflectance of the earth's surface. Thereby, pixels represent the smallest unit depending on sensor resolution. Since the launch of the first civil earth observation satellites in the 1970s, the resolution of satellite sensors has constantly increased. Especially in VHRS images, it is very likely that neighbouring pixels represent the same object or land cover class as the pixel under consideration. The aim of object-based analysis is the cognition and separation of objects that are not completely homogenous in the composite of their pixel values. (Blaschke, Strobl 2001)

The first step in the object-based process is the segmentation of the image with an adequate segmentation-algorithm under consideration of particular criteria of homogeneity. The following classification of the segments is knowledge-based and is performed in a process-tree, where the specific characteristics are expressed in certain formulas and models.

All object-based applications in this thesis were done with the software Definiens Developer 7 from Definiens.

4.6.1 Multi-Resolution Segmentation

The patented segmentation algorithm from the Definiens Developer 7 was developed to work even on highly textured image data and is therefore applicative to VHRS data. This fundamental method is a largely knowledge-free and unsupervised segmentation of homogeneous image objects primitives in any selected resolution.

The multi-resolution segmentation algorithm successively merges pixels or existing image objects. Thus, it is a bottom-up segmentation algorithm based on a pair-wise region merging technique. Multiresolution segmentation is an optimization procedure, which minimizes the average heterogeneity and maximizes their respective homogeneity for a given number of image objects. The segmentation procedure works according to the following rules, representing a mutual-best-fitting approach:

- The segmentation procedure starts with single image objects, called seeds, of one pixel size and merges them in several loops iteratively into pairs to larger units as long as an upper threshold of homogeneity is locally not exceeded. This homogeneity criterion is defined as a combination of spectral homogeneity and shape homogeneity. The calculation can be influenced by modifying the scale parameter. Higher values for the scale parameter result in larger image objects and smaller values in smaller image objects.
- As the first step of the procedure, the seed looks for its best-fitting neighbour for a potential merger. If best-fitting is not mutual, the best candidate image object becomes the new seed image object and finds its best fitting partner. When best fitting is mutual, image objects are merged.
- In each loop, every image object at the image object level will be handled once.
- The loops continue until no further merger is possible.

(Definiens AG 2006)

4.6.2 Parameters for Multi-resolution Segmentation

The homogeneity criterion of the multi-resolution segmentation algorithm measures how homogeneous or heterogeneous an image object is within itself. The homogeneity criterion is calculated as a combination of colour and shape properties of both, the initial and the resulting image objects of the intended merging. Here, the colour homogeneity is based on the standard deviation of the spectral colours, whereas the shape homogeneity is calculated on the deviation of a compact or a smooth shape. The homogeneity criterion can be customized by weighting shape and compactness criteria. The weighting of colour and smoothness criteria is derived from the complementary weighting (see Figure 14):

- The weighting w1 is set of shape within the homogeneity criterion between 0.1 and 0.9.
- The weighting of colour assumes a value so that colour and shape sums up to 1. That means, the weighting of colour is (1–w1).
- The weighting of w2 sets the compactness within the shape criterion between 0.1 and 0.9.
- The weighting of smoothness within the shape criterion assumes a value so that smoothness and compactness sums up to 1. That means, the weighting of smoothness within the shape criterion is (1–w2).

(Definiens AG 2006)

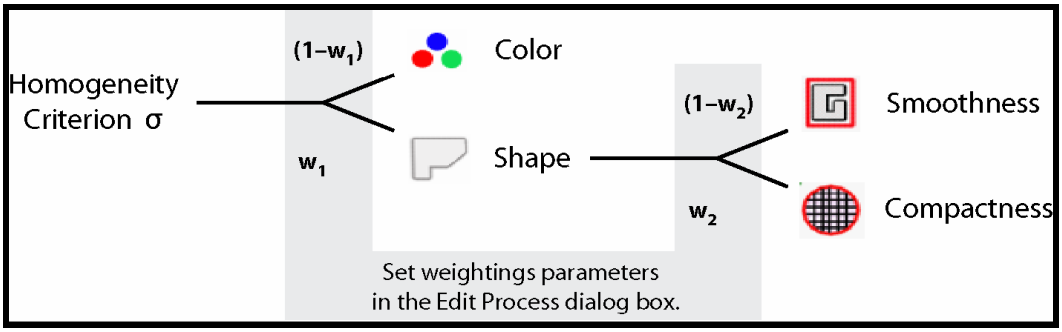

Figure 14: Weighted components of the homogeneity criterion in the Definions Developer
Source: (Definiens AG 2006)

The values were tested and varied regarding to the best homogeneity for bright looking shelters for the object-based classification of Amnabak and Koubigou. The mentioned shape-criteria was set at 0.4, which results in 0.6 for the weighting of colour. For compactness, 0.9 was chosen, which entails 0.1 for smoothness. Uttenthaler et al. 2007 recommended to mind that the bright reflectance of dwellings have high values in the blue band. Therefore, the weighting for used bands for the multi-resolution was set at 2 for the blue band and at 1 for the red, green and infrared band. That places emphasis on the blue band twice during the segmentation process.

The resulting segments (see

Figure 15) showed a good homogeneity for shelters marked out to the surrounding environment.

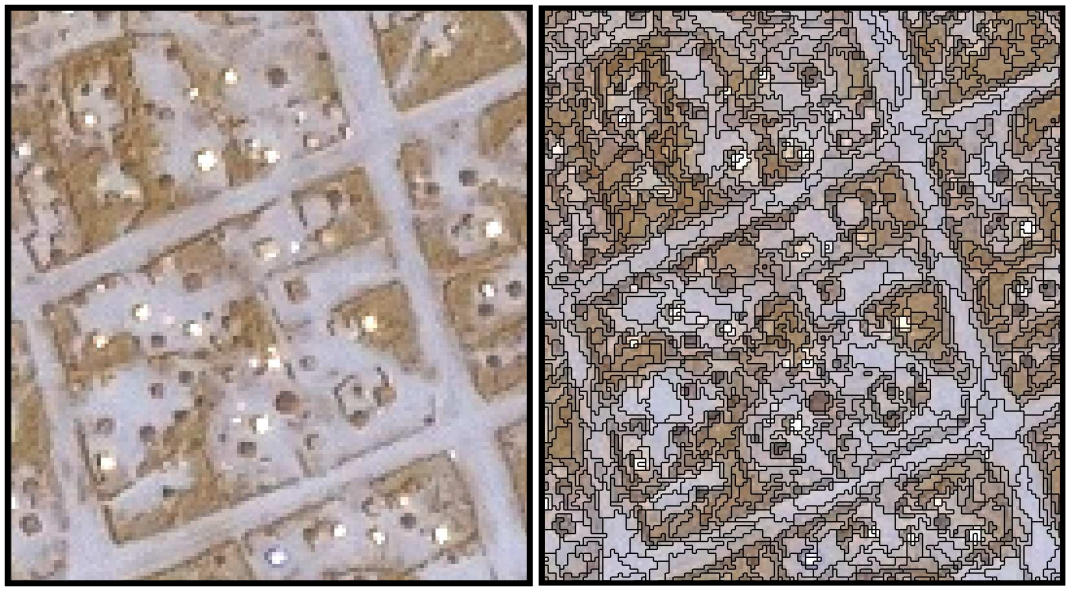

Figure 15: The left image shows a part of the campsite Koubigou, before and the right image after multi-resolution segmentation. Pixels were segmented regarding to the mentioned homogeneity criteria.

4.6.3 Object-Based Analyses

There are numerous options for carrying out object analysis and classifications in Definions Developer 7 and there is no prescribed way to do it. In the approach from Uttenthaler et al. (2007), who analysed informal settlements in Zimbabwe, more than the settlement-class were categorized. He took different shapes and areas into account and differentiated objects to each other with thresholds and

their relations to neighbouring objects. On the other hand, Giada's et al. (2003b) approach extracted shelters in refugee camps in Tanzania. Fuzzy classifications were applied between the shape, size and spectral signatures of classified objects. These are just two examples of the possibilities of object analysis in Definions Developer 7.

In this thesis, the aim was a transferable analysis to extract bright reflecting shelters of the campsites Amnabak and Koubigou. After the segmentation process, the segments were examined in shape, size, tone and pattern regarding to their neighbouring objects. It was found out that neighbouring segments of the bright shelters in both campsites had a lower tone than the bright shelters. Moreover, the size and pattern of the segments representing shelters were similar to the results that were observed during the visual interpretation in chapter 4.2. Based on that, a rule set for the classification was implemented in the process tree.

4.6.4 Object-Based Classification

Single processes are the elementary units of a rule set providing a solution to a specific image analysis problem. To build up a rule set for the object-based classification, every single process has to be edited. An algorithm has to be executed on the image objects. By combining single processes in a sequence, a process sequence is organized with parent and child processes, which are executed in a defined order. Developing a rule set is a concept applicable within the graphical user-interface, called process tree. (Definiens AG 2006)

The rule set which was built up is transferable to both campsites with just marginal modifications and contains the following sequences (several steps of the sequences are displayed in Figure 16):

- A multi-resolution segmentation with the parameters described in chapter 4.6.2 was applied to the images Amnabak and Koubigou (see Figure 16, number 1 before segmentation and number 2 after segmentation).
- A rule to merge all segments with neighbouring objects that have an average difference in the reflectance that is smaller than 50 units for Amnabak and smaller than 100 units for Koubigou. That ensures the on-

going separation of the bright reflecting shelters to the surrounding segments (see Figure 16, number 3). This was looped three times to get a high separation of shelters to all other objects. Note that the average difference is calculated again for every merged object per loop.

- All remaining objects, which were higher in the average difference of the reflectance than their neighbouring segments, were classified as shelters (see Figure 16, number 4). For Amnabak, the values were set at 100 and for Koubigou at 40.
- All neighbouring shelters were merged (see Figure 16, number 5).
- Shelters with a difference to their unclassified neighbours of less then 150 units were removed from the class shelters.
- Shelters with areas more than 22 square meters for Amnabak and Koubigou and with less than 2 for Koubigou, and 4 square meters for Amnabak were removed from the class shelters (see Figure 16, number 6).
- All shelters outside the campsites were removed due to using the GIS-based grid-cells that were developed during the visual interpretation (see chapter 4.2).
- All remaining shelters were exported into a point-vectorlayer for further statistical analysis and comparison with the reference data in a GIS.

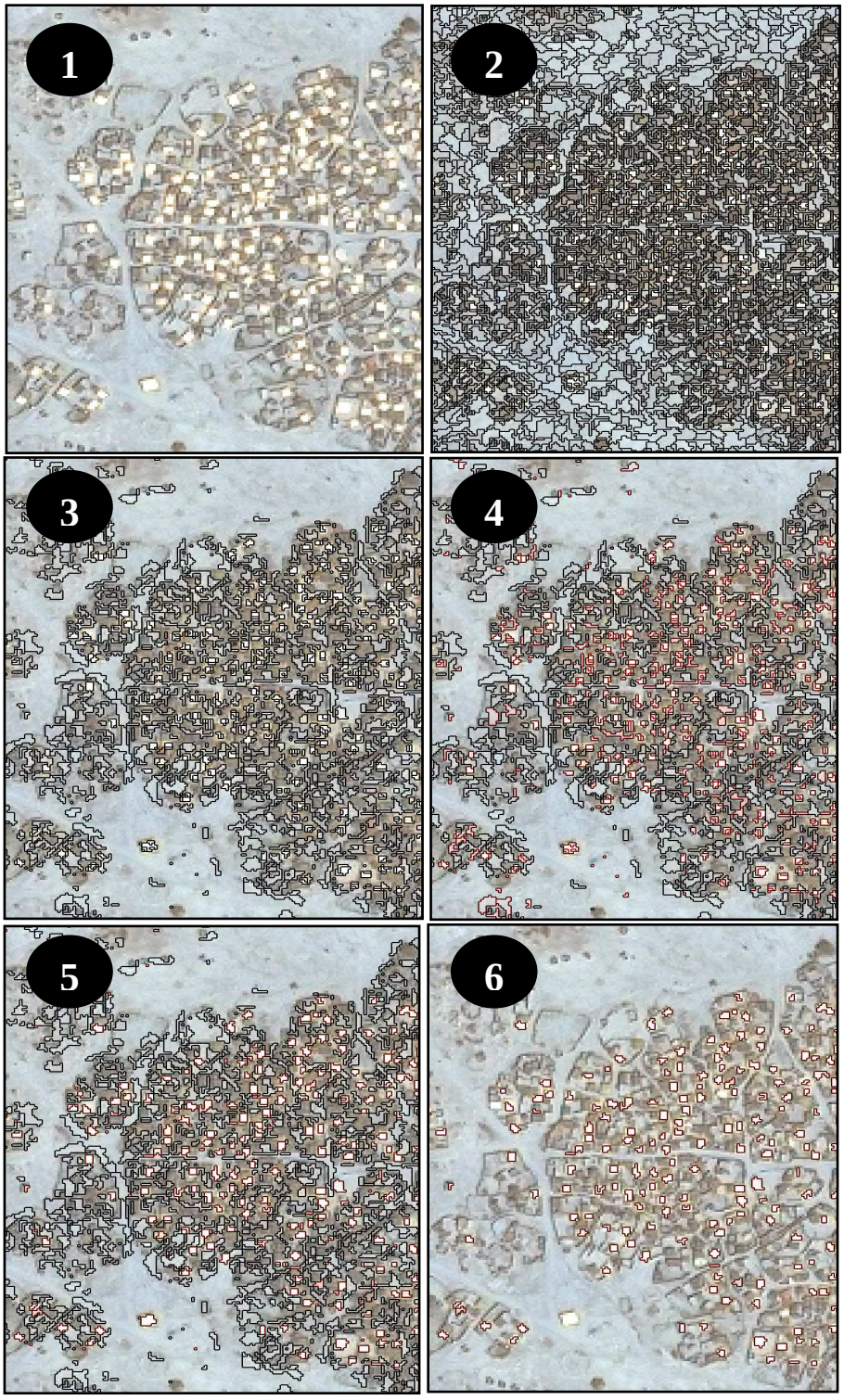

Figure 16: Exemplary screenshots for object-based classification in the image Amnabak. 1. Image before segmentation; 2. after segmentation; 3. merging of similar neighbouring objects; 4. classification of shelters; 5. merging of objects in class shelters; 6. final shelter objects after area thresholds.

4.6.5 Results of Object-Based Analyses

The first column in Table 17 and Table 18 shows the results of the object-based classifications that were counted automatically in Definions Developer 7 as well as the visually interpreted reference data. The user's accuracy, producer's accuracy and overall accuracy were achieved in the same way as shown in chapter 4.5.4 following the adjusted guidelines from Congalton (1991).

Table 17: Statistic of object-based methods for Amnabak

Classification methods	Identified Shelters	Correctly identified shelters	User's accuracy	Producer's accuracy	Overall accuracy
Visual	2158	--	--	--	--
Object-based	2128	1965	92.34 %	91.06 %	85.66 %

Table 18: Statistics of object-based methods for Koubigou

Classification methods	Identified Shelters	Correctly identified shelters	User's accuracy	Producer's accuracy	Overall accuracy
Visual	500	--	--	--	--
Object-based	565	434	86.80 %	76.81 %	68.78 %

5 Possibilities of TerraSAR-X for Refugee and IDP Camp Mapping

Due to recent availability of the data (see chapter 3.6), scientific approaches for the analysis of refugee and IDP camps with very high-resolution radar imagery are still at the beginning. In the following chapters, the radar data are observed concerning the recognisability of important features that would be meaningful for refugee and IDP camp mapping. Additionally, several filtering techniques will be implemented to reduce speckle and enhance the interpretability for the viewer.

5.1 Filter Techniques for a TerraSAR-X Spotlight Image of Amnabak and Koubigou

The spotlight images of the camps were directly compared to the spatially identical IKONOS data. That was done in the delivered state without filtering techniques and with several filtered images. The aim was the comparison of the enhancement of particular filter techniques according to the studies of Herold, Haack 2001, who applied filters to reduce speckle in images received from the Canadian radar remote sensing satellite Radarsat-1.

The ERDAS IMAGINE Radar Interpreter application offers several filter algorithms for speckle reduction, edge and image enhancement and texture analysis. All filters were tested in respect to better contrast, edge enhancement and differentiation of objects in the images. In the same context, as already mentioned in chapter 4.2, the interpreter interactively decides which filter algorithm and window size is best for the used data and aimed application. (ERDAS 2005)

All available filters of the ERDAS IMAGINE Radar Interpreter were applied and examined on the radar images. In contrast to Herold and Haack (2001), who had best results with a successive 5x5 median 21x21 variance filter, the following conclusions were made:

- For speckle reduction, Lee (already mentioned in Figure 7) and Gamma filters (see Figure 17) were assumed to be most effective for a better

contrast. That was done with a 3x3 and 5x5 moving window and the associated Coefficient of Variation.

- Edge and image enhancement applications showed no appreciable improvement to the data.
- Best results due to the discrimination of single objects were achieved with a texture analysis with 3x3 and 5x5 moving windows. The algorithms were variance (2nd-order), skewness (3rd-order) and kurtosis (4th-order). For optimal visualization the resulted images were combined into a 3-colour RGB (Red-Green-Blue) image (see Figure 17).

Compared to Herold and Haack 2001, the different outcomes arise probably from the diverse sensor attributes and the higher spatial resolution of TSX. Note that filtering techniques always have to be modified regarding to radar sensors and the specified aims of studies.

5.2 Fundamentals for the Interpretation of Radar Data

Radar images can differ much compared to optically received images in respect to active image acquisition and other characteristics of radar remote sensing that were already described in chapter 3.5. Hence, the image interpreter must always keep in mind that the radar sensor “sees” the earth surface under other conditions than he himself. The black and white radar image displays the backscattered microwaves that were modified by roughness, dielectric properties and slope of the sensed objects in different grey levels. Thus, following attributes of tone, size, shape, structure and texture in radar images should be specified in respect to differences of the interpretation of optical images (see chapter 4.2):

- The tone in radar imagery can be seen as the average intensity of the backscattered signal. High intensity returns appear as bright tones on a radar image, whereas low signal income emerges as dark tones. For example, most urban areas have a very strong backscatter, forests have medium backscatter and calm water has almost no backscatter.

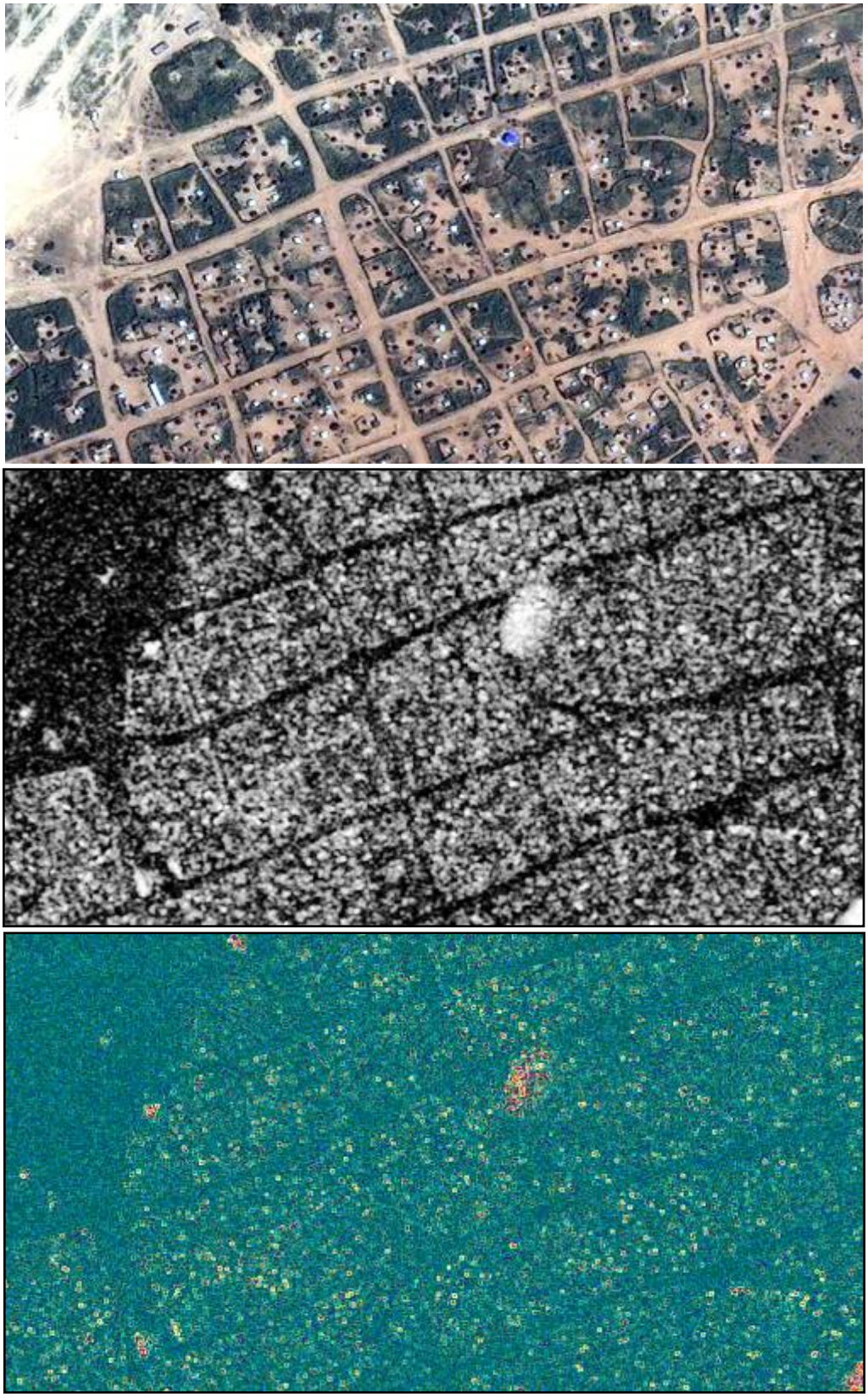

Figure 17: Different highlighted satellite images of the Koubigou camp showing the same location. The upper image was received from IKONOS.. The medium image is 5x5 Gamma-filtered and the lower image shows RGB-composite of three texture filters with red for variance, green for skewness and blue for kurtosis.

- The shape can be defined as a spatial form regarding a relative constant contour or periphery, or the object's outline. Some features like i.e. streets, residential areas or bridges can be distinguished by their shape. It should be mentioned that the shape is as seen by the slant illumination, which comes from a certain direction, i.e. right-looking.
- The structure is the spatial alignment of features over an area with a recurring arrangement.
- The size of objects in the radar image can be used as a qualitative component for identification. The size of known features like i.e. houses or fields in the image gives an impression and a comparison of the extent as well as proportions of other features in the region.
- The texture in a radar image can be divided into the three levels of micro-, meso-, and macro-texture.
- The micro-texture has at least the size of a resolution cell in the image and is difficult to interpret due to speckle noise. Speckle is a typical characteristic of a radar system and is not directly connected to the properties of the recorded scene.
- The meso-texture is also called scene-texture and is useful for radar interpretation. It shows the natural difference of average backscatter to an extent of several resolution cells. Therefore, meso-texture is an expression of slope and elevation changes or the canopy structure of vegetated areas depending on the spatial resolution of the system.
- The macro-texture is the variation of resolution cells over the entire image and helps to delimit geomorphic or geologic as well as landuse regions. Examples for that could be fields, drainage patterns, mountains and streets.

For further reading about interpretation of radar imagery and related interacting effect, see the detailed descriptions in Henderson and Lewis 1998 and find additional information online at the Earthnet[6] from ESA.

[6] http://earth.esa.int/

5.3 Visual Interpretation of the Campsites

The analyses of the images were done with a large scale level for the macro-texture of 1:6.000 and small scale level for scene-texture of 1:1.000 to examine interpretable features of the filtered and unfiltered TSX images. For validation of the interpretation, the optical images received from IKONOS were traced with a blending or swiping method above the radar images.

5.3.1 Visual Analysis Amnabak

At a large scale level, Amnabak (see Figure 18) campsite could be identified in contrast to the outlines of its residential areas. The structure of the residential areas regarding to the path-lines and the accumulation of shelters are also cognizable. Around the camp, several fences and trees along the wadis are interpretable.

At a small scale level, several objects could only be distinguished with filtered images. The RGB-texture filtered image showed high values that were point-like in the residential areas and dotted outside the camp. After the implementation of the blending method combined with the optical image it was found out, that these points partially represent shelter and the surrounding living structures inside the camp as well as trees outside the camp and within the village. Buildings that were interpreted from IKONOS images as structures from relief organizations and village houses could also be distinguished because of very high backscatter. Lee and Gamma-filters disclosed larger structures like block-shaped residential and fenced areas.

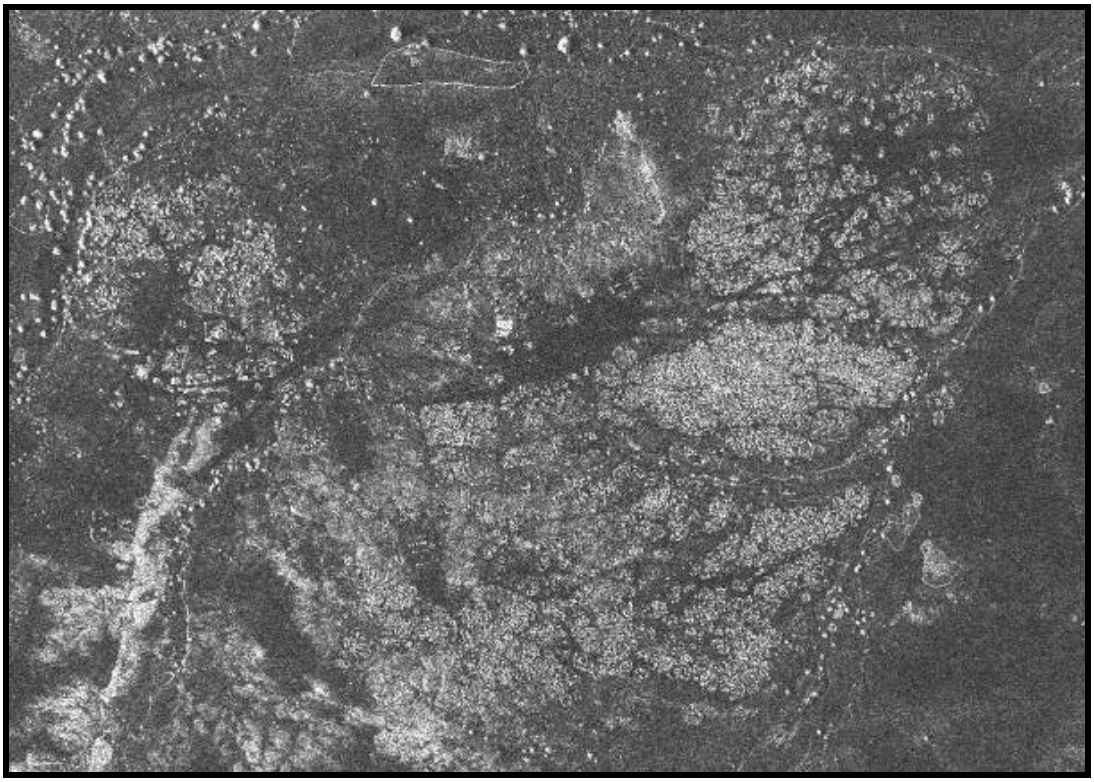

Figure 18: TerraSAR-X high-resolution spotlight image of Amnabak. The camp is cognizable due to high backscatter in the central-eastern part of the image. Around the camp several fences and trees along the wadis are visible. The village of Amnabak in the west also appears bright.

5.3.2 Visual Analysis Koubigou

At a scale of 1:6.000, the northern and southern hills around Koubigou (Figure 19) are cognizable due to high backscatter probably caused by coarse underground. Also, typical drainage structures of wadis in the east are visible. Streets and paths are perceptible like in Amnabak, but there is no sharp outline from residential areas to the environment. That is probably due to more consistent vegetation in and outside the camp. Bigger trees westerly within the village of Koubigou also appear bright in the image.

At a smaller scale of 1:1.000, it was again not possible to differentiate single objects without applied filters like in the image of Amnabak. The visibility of the features like trees, shelters and buildings were best with texture filters and also Gamma and Lee-filters showed good contrast for residential areas and streets.

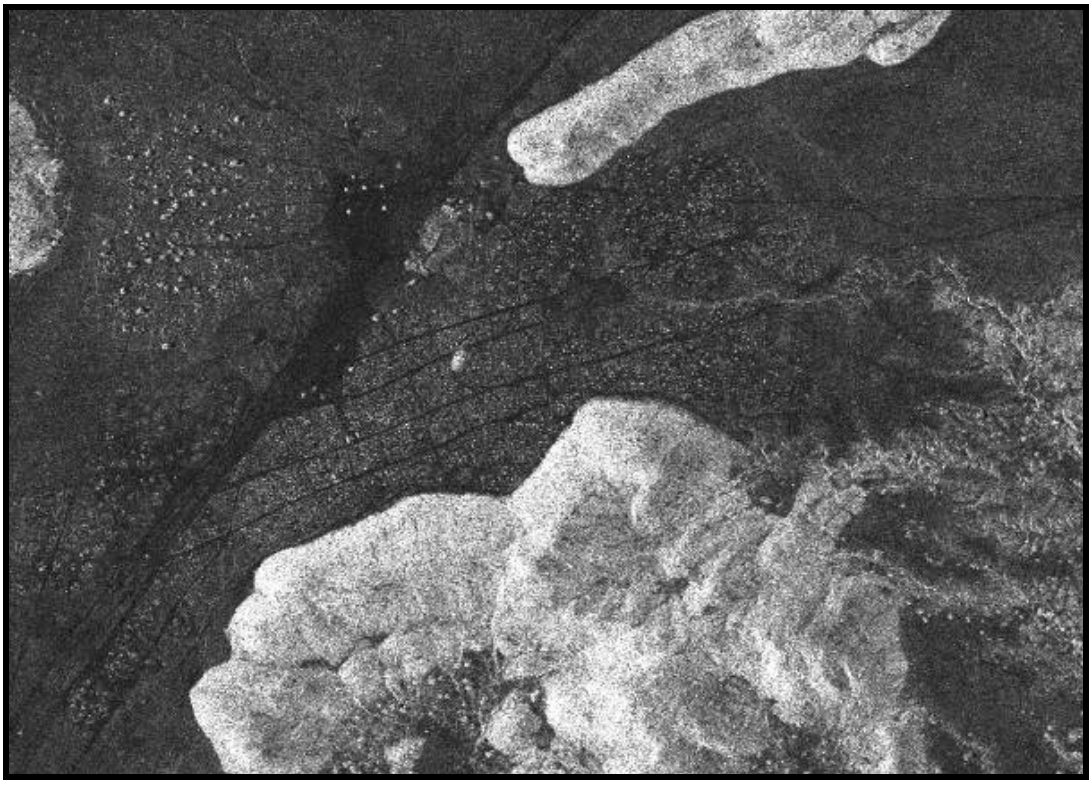

Figure 19: TerraSAR-X high-resolution spotlight image of Koubigou. Hilly terrain in the north and th south appear bright. In the eastern part a wadi drainage system is recognisable as well as tree vegetation in the village of Koubigou in the west. Also, streets and paths within the campsite in the centre can be distinguished from residential areas by partitioning them.

5.3.3 Shelter Extraction with TerraSAR-X Data

In both TSX images, the white shelters, which were previously identified and digitized through IKONOS data (see chapter 4.3.1) and whose extraction was meant to be the main goal of this thesis, could not be definitely recognized and separated from other features in the image. It was assumed that the material of the white shelters are probably penetrated by X-band microwaves and for that reason, reflections arise from the underground. That could be due to a low dielectric constant of the material or the attributes of backscatter, received from the dwellings, have just no significant varieties from the surrounding ground. At a larger scale, the backscatter of a residential area, which means the near surrounding area of a shelter, has a high backscatter but that was not strictly associated geographically to shelters. Resulting from internet research, pictures of Amnabak, which were found, showed that the building material around the shelters with white roof top was dry clay with some straw, which could cause the

mentioned reflection. That was additionally validated through an email-correspondence to a former humanitarian relief worker in Amnabak.
In the texture filtered images of TSX, several point-like objects appear (see Figure 17, bottom image) within the position of features that could previously not exactly be identified through the IKONOS image (see chapter 4.2). That means, it was not possible to interpret these features as huts or as objects with a vertical extent. Regarding the intensity of the backscatter in the TSX imagery, these objects could be kinds of dwellings probably build from local material without plastic sheets on the rooftop.
Furthemore, it was tested if the combination of both, radar and optical image, could bring any benefit to the interpretation in respect of mapping both, bright and dark, huts.

5.4 Combined Approach of TerraSAR-X and IKONOS Data

Blaschke et al. expected 2007 an improvement with a combined approach of TSX with optical VHRS data in i.e. the cognition of rooftops in refugee camps. With simultaneous consideration of the filtering techniques in chapter 5.1 and the visual interpretation of the campsites along with the previous assumptions in chapter 5.3.3, the approach of radar and optical data was tested. The approach followed the studies of Herold and Haack (2001), who combined Landsat (7 bands) with filtered Radarsat data (1 band) into imagery with eight bands for supervised classifications. In respect to the different sensor attributes of TSX and IKONOS and a visual interpretation method, the approach from Herold and Haack (2001) was modified. Four bands from IKONOS were combined with the unfiltered and also with the texture-filtered image from TSX to 5-band images in each case. Those layer stacks were then analysed for optimal band display due to the enhancement of feature identification and additional information about the environment. The satellite data from IKONOS as well as from TSX are geo-rectified at a high precision level and matched identically to each other, which is an important precondition. The temporary matching of the images is about six months apart from each other, which implements an uncertainness that could not

be compensated due to missing up-to-date optical VHRS imagery and current ground truth data.
At that point, it has to be noted that the following conclusions in the subchapters are assumptions on experience in image interpretation based on previous studies and appropriate literature. The following assumptions can be taken as a hypothesis for further research but not for validation of the classification.

5.5 General Assumptions for a Combined Approach

For both scenes, the RGB combination of the bands blue, NIR and unfiltered radar (see Figure 20 and Figure 21) showed the best results for supplementary image information in respect to the discrimination of geomorphic and geologic characteristics.

- Residential areas with high backscatter were detected by radar and were displayed noticeably in the image.
- Buildings in the villages of Amnabak and Koubigou appeared clearly.
- Trees and fences along the wadis and inside and around the villages came out in a very obvious shape.
- Coarse underground in Amnabak, probably due to fluvial erosion, which was already assumed in chapter 4.3.3., could be identified.
- Hilly terrain in Koubigou was represented by a clear outline in comparison to its surrounding environment.
- Vegetation was more distinguishable into high and low vegetation canopy i.e. sparse vegetation was more displayed in NIR and tree and bush vegetation through radar backscatter.

The main benefit of the included radar band was the highlightening of vertical structures, slope and coarse underground and the discrimination of vegetation supported by the NIR.

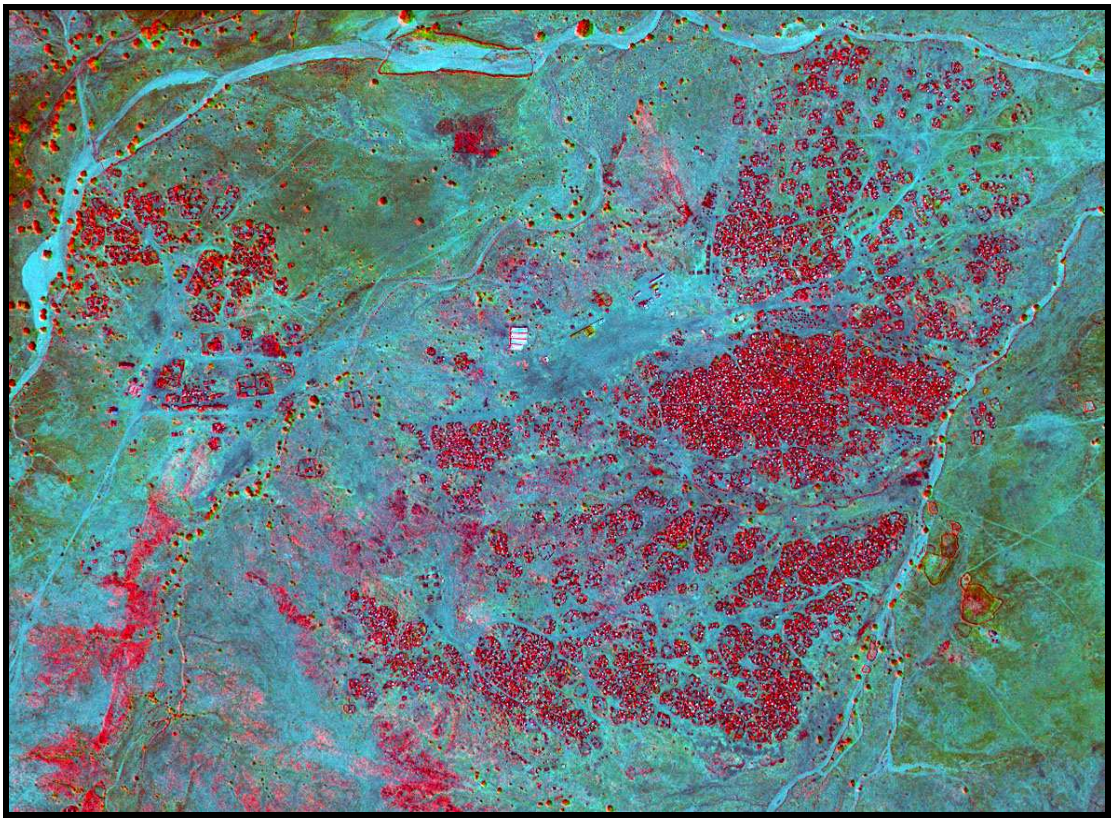

Figure 20: Layer stack of IKONOS combined with TerraSAR-X data from Amnabak. The blue and NIR band of IKONOS in and the unfiltered radar-image from TerraSAR-X got displayed in RGB with radar band in red, the NIR in green and the blue band in blue.

Furthermore, the RGB combination of the bands blue, NIR and variance-filtered radar (see Figure 22) showed advantages for additional feature identification.

- The white shelters were still differentiable to their surrounding environments.
- Dark appearing features that were assumed to be huts or other shelters also showed partially high values on the (variance-) radar band in Koubigou campsite and could be identified as features with a vertical structure.
- Bigger buildings that were assumed to be in use of humanitarian relief organisations were partially highlighted by the radar band.
- Hilly terrain was still emphasized.
- Fences and underground did not get accentuated any more, what provides less confusion for the analyst.

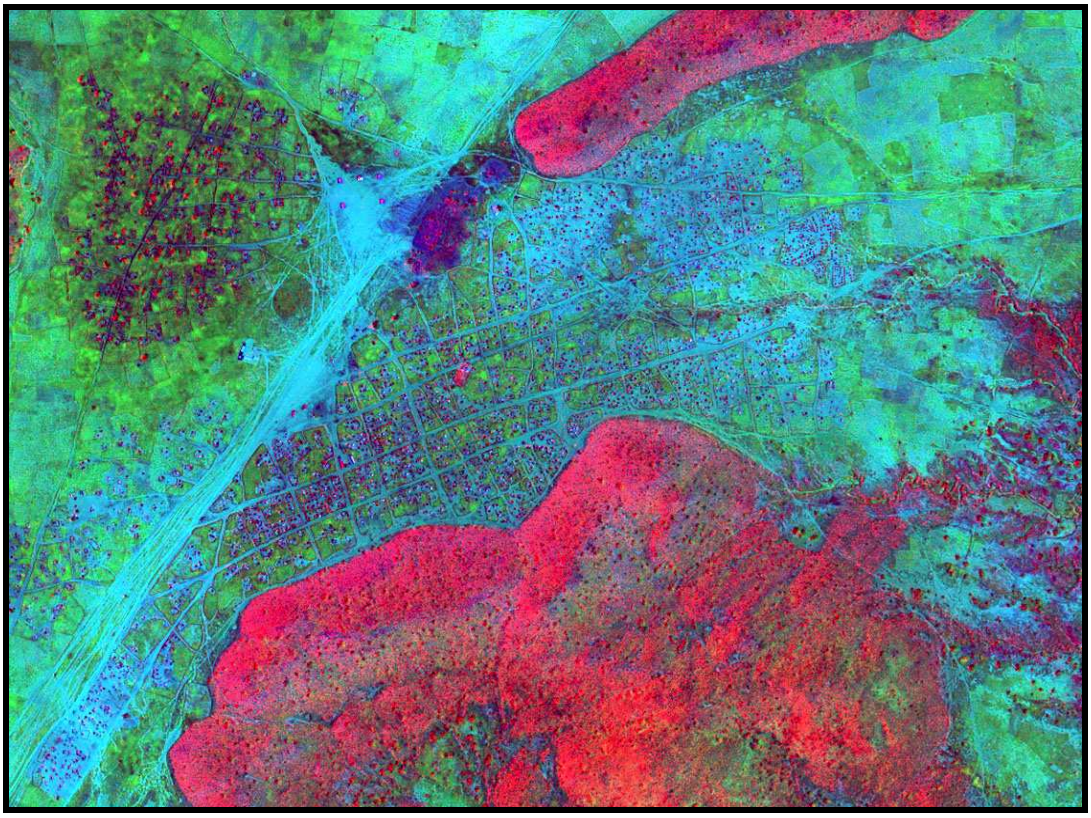

Figure 21: Layer stack of IKONOS combined with TerraSAR-X data from Koubigou. The blue and NIR band of IKONOS in and the unfiltered radar-image from TerraSAR-X got displayed in RGB with radar band in red, the NIR in green and the blue band in blue.

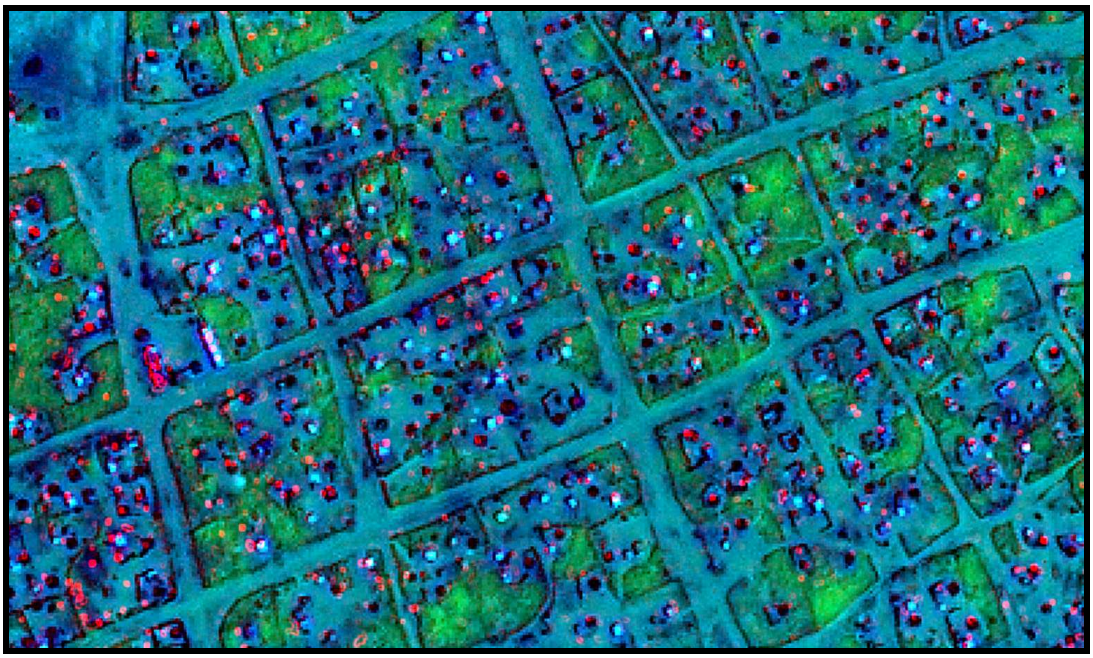

Figure 22: Enlarged part of the layer stack of IKONOS and TerraSAR-X data from Koubigou. The bands of IKONOS blue and NIR and the variance-filtered radar-image from TerraSAR-X, displayed in RGB with radar band in red, the NIR in green and the blue band in blue.

The major advantage of this layer combination was the possibility of additional shelter extraction of the previously unsure dark features i.e. if high values from the texture (variance) filtered radar band overlaps with dark features displayed by IKONOS data. It has to be noted that due to the geometrical effects of side-looking radar the aimed targets can be shifted away to a certain extent from the same object in the overlapping optical image which is recorded from a central perspective.

6 Discussion

In the following sub-chapters, the results of the methods for refugee and IDP camp mapping will be discussed focusing on shelter extraction and their potential of implementation in diverse situations. Furthermore, future recommendations will be given to refine the techniques with respect to future trends in remote sensing and classification methods as well as for interactions with the end-users of the extracted information.

6.1 Comparison for Shelter Extraction Methods

The evaluation of several methods with the purpose of a most accurate extraction of shelters in the refugee camp Amnabak and the IDP site Koubigou is carried out for both places simultaneously. Moreover, the results are discussed in terms of the differences that arose with dissimilar methods and camp characteristics. The accuracy of shelter detection was generally higher in Amnabak than in Koubigou, which was due to the better separation of the bright appearing shelters in Amnabak. In order to sum up the results for shelter extraction methods, the accuracy assessment of all methods is listed again in Table 19 and Table 20.

The performance, which entails the lowest stability in outcome was the *Unsupervised Classification*. In Amnabak, the overall accuracy was 87.22 %, but the very high difference to the overall accuracy in Koubigou with 34.60 % shows that the quality of the method strongly depends on the characteristics of the aimed features. The analyst's impact on the ISODATA algorithm (see chapter 4.4.2) of the *Unsupervised classification* is of little relevance and refers mainly to the definition of the number of classes that are created. Thus, the intended features have to be in a unique spectrum, which enables the ISODATA algorithm to separate them from other classes in the imagery. This was the case in Amnabak but not in Koubigou, where the bright appearing shelters contained more complexity in their reflection. However, the *Unsupervised Classification* has the great advantage of its rapidness. The technique can be implemented on an image within a couple of minutes due to the small amount of parameters that have to be

set up. In addition, the accuracy and transferability of the method increases with the homogeneity and exclusivity of the reflected spectrum of the shelters.

The *Threshold Classification* (see chapter 4.4.3) technique showed more stable results for both images than the *Unsupervised Classification*. The overall accuracy was 75.01 % for Amnabak and 65.43 % for Koubigou. The differences came up due to the same reasons discussed at the beginning of the chapter. Once the performance is set up in Knowledge Engineer in ERDAS IMAGINE, the upper and lower margins of the thresholds can simply be inserted. Concerning the transferability of the *Threshold Classification*, the values for the spectral profile have to be taken each time again for new satellite imagery. The time consumption for that depends on the number of testing points for the spectral profiles, which is therefore also interconnected to the accuracy of the threshold ranges. That means with increasing testing points, the range of the thresholds gets more precise for the reflecting sunlight from shelters in the campsites. One benefit of *Threshold Classification* is the transferability to other features, which could be i.e. dark appearing shelters. Compared to the *Unsupervised Classification*, the aimed class can also be specified as a spectrum, which is quite exclusive in the image. The inherent limitation of this technique is the need of homogeneity of the shelter reflection in that specified application. A future refinement of this method could be the merging of several threshold ranges to get a broader amount of different shelters.

With overall accuracies of 88.43 % for Amnabak and 62.59 % for Koubigou, the *Supervised Classification* achieved robust results for both images. This method also depends on spectral profiles, which have to be taken again for every new scene. Besides the shelter class, other classes can be defined additionally. The temporal effort for that technique depends on the aimed correctness of the examined spectral training areas and the number of classes that are intended. Pertaining to the characteristics (see chapter 4.4.1) and the accomplished results, the *Supervised Classification* can be seen as the best pixel-based classification method if time consumption is no limiting factor. The ability to extent and define

more classes to examine a scene emphasizes this technique for future studies, when more aspects of refugee and IDP camps are getting analyzed.

Also, the *Object-based Classification* yielded robust results with an overall accuracy of 85.66 % for Amnabak and 68.78 % for Koubigou. These results were similar to the results of the *Supervised Classification*. In contrast to the pixel-based methods, the object-based technique defines characteristics of the required class by means of the perception of the viewer (see chapter 4.6.4), i.e. regarding size, shape etc. Once the required process tree is defined, the transferability of this technique increases, the more general the extraction process is defined, i.e. for the implementation of the process tree for Amnabak to Koubigou, only three parameters have been modified. Thus, time consumption for the extraction process is of no consequence as soon as the process tree is defined. Concerning these aspects, the *Object-based Classification* shows the best performance in broad use for shelter extraction methods. In respect to increasing spatial resolution of remote sensing satellites and the ability for classification of that data, this method is discussed again at a later point.

The number of shelters from the *Visual Interpretation* was accepted to be used as reference data for validation of the shelter extraction methods after the previous mentioned approaches of Giada et al. (2003b) and Lang et al. (2006). Apart from the highest accuracy of all methods, time consumption can be discussed as a controversial component. On the one hand, it took between 1.5 – 2.5 h to digitize between 500 – 2158 white shelters from the imagery, which is adequate due to the high accuracy. On the other hand, time sums up proportionally to the amount of shelters in a camp, which shows the difficulty for visually achieved extraction if the camp size reaches a critical number, i.e. the former refugee camp Hartisheik[7] in Ethiopia hosted up to 250,000 people which should be complicated to map visually.

[7] http://www.unhcr.org/cgi-bin/texis/vtx/news/opendoc.htm?tbl=NEWS&id=40e426de4 (16.06.2008)

For the use of the TSX images the *Combined Approach* with IKONOS and TSX displayed the best results. A visual interpretation showed that the counting of bright shelters could still be achieved with the same characteristics described in the prior passage about the Visual Interpretation of the IKONOS image. The advantage of the *Combined Approach* compared to all other methods is based on the assumption that additionally dark appearing dwellings could be defined through radar backscatter (see chapter 5.5) from vertical structures. For that purpose, further research should be carried out to examine the correct camp structures for valid ground truth. Then, modifications of the pixel-based and object-based techniques could be tested on the combined imagery.

Table 19: Results of all methods for shelter extraction methods applied on the IKONOS image of Koubigou

Classification Methods/ Koubigou	Identified Shelters	Correctly identified shelters	User's accuracy	Producer's accuracy	Overall accuracy
Visual (reference data)	500	--	--	--	--
Supervised	604	425	85.00 %	70.36 %	62.59 %
Unsupervised	877	354	70.80 %	40.36 %	34.60 %
Threshold	481	388	77.60 %	81.67 %	65.43 %
Object-based	565	434	86.80 %	76.81 %	68.78 %

Table 20: Results of all methods for shelter extraction methods applied on the IKONOS image of Amnabak

Classification Methods / Amnabak	Identified Shelters	Correctly identified shelters	User's accuracy	Producer's accuracy	Overall accuracy
Visual (reference data)	2158	--	--	--	--
Supervised	1978	1941	98.13 %	89.94 %	88.43 %
Unsupervised	1987	1931	97.18 %	89.48 %	87.22 %
Threshold	2372	1942	89.99 %	81.87 %	75.04 %
Object-based	2128	1965	92.34 %	91.06 %	85.66 %

6.2 Implementation of Shelter Extraction Methods

The following chapter gives recommendations for several implementations of methods for shelter extraction in diverse circumstances in refugee and IDP camps. Varying demands (see chapter 2.4) in diverse phases of camps will be discussed depending on the characteristics of the methods in regard to time and accuracy. As briefly described in chapter 2.4.2, the phases in camps can be divided into an *emergency* phase, a phase of *care* and *maintenance* and a phase of *reparation*. Depending on the situation, diverse geo-information is required for humanitarian relief organizations or policy makers.

During an *emergency* phase the determining factor is time. In any crisis, where satellite imagery is used, techniques for fast response are of high interest. Such circumstances eventuate when no useful information can be acquired from the ground due to the remoteness of area or a potential threat, i.e. natural dangers or armed conflicts. That was the case when the civil war started in the Darfur region in Sudan. Within a short period of time, the populations of refugee camps in Chad doubled and it was not possible to get accurate data from the ground to manage the supply of aid. Those camps were not supervised through humanitarian relief

organisations at that time. During that *emergency* phase the "Center for Satellite Based Crisis Information" (ZKI), which is a service of DLR's (German Aerospace Centre) German Remote Sensing Data Center (DFD), provided the UNHCR with rapid acquisition, processing and examination of VHRS data for the estimation of the numbers of shelters in two refugee camps in Chad.

Due to the results of the applied methods in this thesis, the best approach for immediate shelter extraction in refugee or IDP camps is given by the *Unsupervised Classification* to get a first impression of the situation quickly. However, this method's limitation becomes evident when the colour of the shelter is not consistent throughout the campsites. Then, a *Visual Interpretation* can be applied to get a higher accuracy. The deficit of that method is with very large camps when visual counting gets too time-consuming and can not be done accurately any more. An implementation of an *Object-based Classification* would be meaningful if a basic process tree is already set up and could be modified quickly regarding the examined image. In national and international organisations, which provide necessary geo-information, these methods are called rapid mapping. The combination of these fast methods also allows an opportunity for a higher accuracy.

Care and *maintenance* of camps is needed to update the information about structure, population and population density of camps. That can be continually done in certain timeframes. As an example, UNHCR has a high interest in long-term changes at campsites in order to refine their methods of assistance. High accuracy is needed for example to improve the supply of camps or for accurate information of the changes in camp structures. Interconnections due to the moving of refugees or IDPs between diverse camps can additionally be ascertained in long-term monitoring.

If long-term analyses are required, it can be presumed that more than one camp is getting analysed. For these purposes, the *Object-based Classification* shows the best results in respect to the transferability of the method. The *Supervised Classification* can be implemented if just one particular site is analysed. This approach brings additional high benefits due to further research purposes if, for example, other information besides shelters is necessary, more classes can be set up. For example, statistical analyses of the surrounding environment could be

done through a land-use classification. Both methods can be assisted through *Visual Interpretation* with the previous mentioned limitations of camp sizes but with the advantages for a high accuracy and possible compensation of ground truth.

The third phase of refugee and IDP camps described by Dalen et al. 2000 is the *repatriation* phase. The main objective of that state is the awareness of the environmental circumstances in the refugees' area of origin, i.e. information on potentially available land for agriculture in the refugee's or IDP's homeland. Furthermore, impacts on the surrounding environment in long-term studies can be registered. For that phase, the extraction of shelters is secondary. Applications for population monitoring could be beneficial before the closing-down of campsites due to the management of repatriation. In that case, the same methods, which were recommended for the phase of *Care* and *maintenance*, are appropriate.

6.3 Conclusion and Future Prospects

For humanitarian relief organisations population estimations for refugee and IDP camps are a key-factor for their general logistics. Especially during emergency situations up-to-date information about concerned locations are of high interest. The use of satellite data for that purpose is a sophisticated approach that can support decision making for policy makers and humanitarian relief organisations. The resulted accuracies in this thesis show that VRHS data can already be used for such cases. A RESPOND workshop in Geneva in March 2008 with several NGOs and representatives from UNHCR and UNOSAT (United Nations Operational Satellite Applications Programme) raised the need for more collaboration as one aspect which should entail in a huge benefit. Ground truth for better evaluation of the methods for shelter extraction could improve the accuracies. That might be done if more sharing of relevant data could be agreed and people on-site may be contacted for support.

Also the newest generation of earth observation satellites (WorldView-1) with a spatial resolution of 0.5 meter and higher offer new opportunities for more detailed mapping approaches. More differentiated results are expected from these data for visual interpretation and supplementary object-based methods designate a high

potential due to the ability to define shape and size of diverse settlements in camps with a semi-automatic approach.

As shown in this thesis the *Combined Approach* with IKONOS and TerraSAR-X data indicates the highest potential for advanced shelter extraction methods. This performance was new, due to the arrangement of both, optical and radar VHRS imagery and should be advised for future investigations. In addition to this, the previous mentioned WorldView-1 might further improve this technique for combined shelter analysis.

Although several analyses have been made in the past over a certain region and it is true that ground truth information is still missing. Thus, it might be a good opportunity to carry out a field survey to verify the assumptions that were made in the previous chapters (see 5.4 and 5.5). Of course it should be taken into account that travelling into such crisis regions can be very risky (which highlights the advantages of remote sensing). One possible solution to solve this problem might be the close collaboration with relief organisations working in the area of interest and to receive ground truth information from their field teams.

7 Bibliography

Agence spatiale canadienne (1996): Radarsat Geology Handbook.

Albertz, J. (2001): Einführung in die Fernerkundung. In: Grundlagen der Interpretation von Luft-und Satellitenbildern. Darmstadt

Auswärtiges Amt Deutschland - Federal Foreign Office Germany (2008): Tschad. Länder- und Reiseinformationen.
http://www.auswaertiges-amt.de/diplo/de/Laenderinformationen/01-Laender/Tschad.html. (accessed 20.03.2008)

Bailly, Philipp (2004): Tschad. Forschungsstelle Kriege Rüstung und Entwicklung (FKRE) Arbeitsgemeinschaft Kriegsursachenforschung (AKUF). Universität Hamburg, Department Sozialwissenschaften, Institut für Politische Wissenschaft (IPW).
http://www.sozialwiss.uni-hamburg.de/publish/Ipw/Akuf/kriege/092_tschad.htm.
(accessed 24.03.2008)

BBC NEWS (1 February 2008): Country profile: Chad.
http://news.bbc.co.uk/2/hi/africa/country_profiles/1068700.stm

Bjørgo, E. (1999): Very high resolution satellites: A new source of information in humanitarian relief operations. In: Bulletin of the American Society for Information Science, Year 1999 Oct/Nov.

Bjørgo, E. (2000): Using very high spatial resolution multispectral satellite sensor imagery to monitor refugee camps. In: International Journal of Remote Sensing, Vol. 21, H. 3, P. 611–616.
Bjørgo, E. (2002): Space Aid: Current and Potential Uses of Satellite Imagery in UN Humanitarian Organizations: US Institute of Peace.

Blaschke, T.; Hofmann, P.; Georg, I., et al. (Hg.) (2007): Möglichkeiten und Grenzen der Fernerkundung für das Monitoring und Safeguarding informeller Siedlungen: Eine Synthese (Dreiländertagung SGPBF, DGPF und OVG, DGPF Tagungsband 16/2007).

Blaschke, T.; Strobl, J. (2001): Whats wrong with pixels? Some recent developments interfacing remote sensing and GIS. In: GeoBIT/GIS, Vol. 6, P 12–17.

CAF – Cluster Applied Remote Sensing (24.02.2008): TerraSAR-X Ground Segment Basic Product Specification Document. From German Aerospace Center (DLR), http://www.dlr.de/tsx/documentation/SAR_Basic_Products.pdf, (accessed 09.04.2008).

Collelo, T. (1988): Chad: A Country Study. Washington: GPO for the Library of Congress. http://countrystudies.us/chad/16.htm (accessed 14.02.2008)

Congalton, R. (1991): A review of assessing the accuracy of classifications of remotely sensed data. In: Remote Sensing of Environment, Vol. 37, P. 35–46.

Cue, E. (2007): Feature: Climbing Mt Everest ; how a refugee camp is built. UNHCR. http://www.unhcr.org/cgi-bin/texis/vtx/chad?page=news&id=416cfcc74, (accessed 02.04.2008)

Dalen, Ø.; Johannessen, O. M.; Bjørgo, E.; Babiker, M.; Andersen, G. (2000): Use of ERS SAR Imagery in Refugee Relief. ESA Internal Document: ENVIREF (Contract no. ENV4-CT98-0762).

Definiens AG (2006): Definiens Developer User Guide. 2006, München.

DFD (2008): ZKI. Zentrum für satellitengestütze Kriseninformation. Deutsches Fernerkundungsdatenzentrum. Deutsches Zentrum für Luft- und Raumfahrt. http://www.zki.caf.dlr.de/intro_en.html (accessed 11.06.2008)

Dial, G.; Bowen, H.; Gerlach, F.; Grodecki, J.; Oleszczuk, R. (2003): IKONOS satellite, imagery, and products. In: Remote Sensing of Environment, Vol. 88, H. 1, S. 23–36.

Ehlers, M.; Gähler, M.; Janowsky, R. (2003): Automated analysis of ultra high resolution remote sensing data for biotope type mapping: new possibilities and challenges. In: ISPRS Journal of Photogrammetry and Remote Sensing, Vol. 57, H. 5-6, S. 315–326.

Elachi, C. (1988): Spaceborne Radar Remote Sensing: Application and Techniques: IEEE Press, New York.

ERDAS (2005): ERDAS Field Guide. In: Atlanta, GA: ERDAS Inc.

ESA: Earthnet Online - Radar Course 3. Independence of solar illumination. Herausgegeben von ESA. http://earth.esa.int/applications/data_util/SARDOCS/spaceborne/Radar_Courses/Radar_Course_III/ (accessed 08.06.2008)

Giada, S.; Groeve, T. de; Ehrlich, D.; Soille, P. (2003a): Can satellite images provide useful information on refugee camps? In: International Journal of Remote Sensing, H. Vol. 24, H22. pages 4249 - 4250.

Giada, S.; Groeve, T. de; Ehrlich, D.; Soille, P. (2003b): Information extraction from very high resolution satellite imagery over Lukole refugee camp, Tanzania. In: International Journal of Remote Sensing, H. Vol. 24, H. 22, pages. 4251–4266.

Goetz, S. J.; Wright, R. K.; Smith, A. J.; Zinecker, E.; Schaub, E. (2003): IKONOS imagery for resource management: Tree cover, impervious surfaces, and riparian buffer analyses in the mid-Atlantic region. In: Remote Sensing of Environment, H. 1, P. 195–208.

Henderson, F. M.; Lewis, A. J. (1998): Principles and applications of imaging radar: in cooperation with the American Society for Photogrammetry and Remote Sensing.

Herold, N. D.; Haack, B. N. (2001): Sensor Fusion of Radar and Optical Data Intergration in the Presence of Speckle. In: Conference Paper from American Society for Photogrammetry and Remote Sensing (ASPRS), Vol. 2001, 23-27 April, St. Louis, Missouri, USA.

IDMC - Internal Displacement Monitoring Centre (11.07.2007): Internally displaced in Chad: trapped between civil conflict and Sudan´s Darfur crisis. IDMC - Internal Displacement Monitoring Centre, 11.07.2007. http://www.internaldisplacement.org/8025708F004CE90B/(httpCountries)/69BB2800A93D1374C12571560029544F?OpenDocument (accessed 03.02.2008)

Italian Space Agency (2007a): COSMO-SkyMed SAR Products Handbook. COSMO-SkyMed Mission.

Italian Space Agency (2007b): COSMO-SkyMed System Description & User Guide. COSMO-SkyMed Mission.

Johannessen, O.M.; Dalen, Ø.; Rost, T.; Bjørgo, E.; Andersen, G. L.; Babiker, M. et al. (2001): ENVIREF - Final Report: Environmental monitoring of refugee camps using high-resolution satellite images. In: NERSC Technical Report No. 201.

Köndgen, O. (2004): Tragödie in Darfur. In: KAS-Auslandsinformationen. Konrad-Adenauer-Stiftung e.V., P. 4–16.

Lang, S.; Tiede, D.; Santilli, G. (2006): Beyond sensors and algorithms – an information delivery approach for population estimation in African refugee camps. Zentrum für Geoinformatik Salzburg (Z-GIS). Cairo, Egypt. (6th African Association of Remote Sensing of the Environment Conference (AARSE), Oct 30 - Nov 2), 2006.

Lillesand, T. M.; Kiefer, R. W.; Chipman, J. W. (2004): Remote sensing and image interpretation - Fifth Edition: John Wiley & Sons Ltd Chichester, UK.

ReliefWeb (26 Sep 2007): Central African Republic's quiet conflict uproots more than 290,000.
http://www.reliefweb.int/rw/rwb.nsf/db900SID/EGUA-77FP9Q?OpenDocument,
(accessed 01.04.2008)

Representative of the Secretary-General on Internally Displaced Persons (United Nations; Office for the Coordination of Humanitarian Affairs; Nations, U. (1998): Guiding Principles on Internal Displacement: OCHA.

Sabins, F. F. (1978): Remote sensing: principles and interpretation: WH Freeman and Company.

Schicho, W. (1999): Handbuch Afrika [Band 1]: Frankfurt.

Schneiderhan, T. (2006): Nutzung satellitengestützter SAR-Daten und des CMOD4-Modells zur Untersuchung des lokalen Windfeldes in der Umgebung von Offshore-Windparks. In: Dissertation der Fakultät für Geowissenschaften der LMU München.

Strube-Edelmann, B. (2006): Der Darfur-Konflikt-Genese und Verlauf. In: Wissenschaftliche Dienste des Deutschen Bundestages, Vol. 09.10.2006.

Tobler, W. R.; Survey, G. (1968): Satellite Confirmation of Settlement Size Coefficient: US Dept. of the Interior, Geological Survey.

UN NEWS CENTRE (18 March 2008): Chad: UN agency moves Central African refugees away from border area. Herausgegeben von UN NEWS CENTRE. http://www.un.org/apps/news/story.asp?NewsID=26014&Cr=chad&Cr1=car, (accessed 18.03.2008)

UNHCR (2007a): Handbook for Emergencies. Third Edition.

UNHCR (2007b): IDPs PResence (Draft). Eastern Chad. UNHCR. http://www.unhcr.org/publ/PUBL/46764ffe2.pdf, (accessed 02.04.2008)

UNHCR (2008): Refugees by Numbers 2006 edition. http://www.unhcr.org/cgi-bin/texis/vtx/basics/opendoc.htm?tbl=BASICS&id=3b028097c, (accessed 26.03.2008)

UNHCR - Population Data Unit (PGDS) (Hg.) (2005): Step-by-Step Guide Mapping a refugee Camp, Vol. 23.11.2005. Geneva.

UNHCR CHAD/DARFUR EMERGENCY (March 2008): Camp Locator. UNHCR. http://www.unhcr.org/cgi-bin/texis/vtx/chad?page=camps, (accessed 02.04.2008)

United Nations (Geneva, 28 July 1967): Convention relating to the Status of Refugees. United Nations.

Uttenthaler, A.; Schöpfer, E.; Lang, S. (2007): Veränderungsanalyse informeller Siedlungen in Townships von Harare/Zimbabwe auf Basis von höchstauflösenden

Satellitenbilddaten. Herausgegeben von J. Strobl, T. Blaschke und G. Griesebner. Heidelberg. In: Angewandte Geoinformatik.

Woodhouse, I. H. (2006): Introduction to Microwave Remote Sensing: CRC Press.